

SEL-71-026

Theory and Performance of N-Path Filters

by

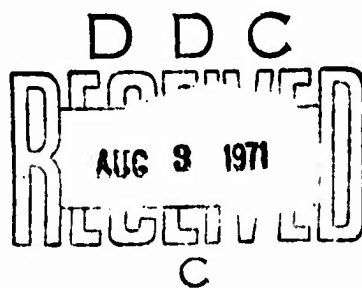
Allston L. Jones

May 1971

This document has been approved for public release and sale; its distribution is unlimited.

Technical Report No. 3602-1

This work was supported wholly by the Joint Services Electronics Program (U.S. Army, U.S. Navy, and U.S. Air Force) under Contract N00014-67-A-0112-0044



RADIO SCIENCE LABORATORY

STANFORD ELECTRONICS LABORATORIES

STANFORD UNIVERSITY • STANFORD, CALIFORNIA

Reproduced by
**NATIONAL TECHNICAL
INFORMATION SERVICE**
Springfield, Va. 22151



AD 222140

13

UNCLASSIFIED

Security Classification

DOCUMENT CONTROL DATA - R & D

Security Classification of title, text, abstract and indexing annotation must be entered when the overall report is classified.

1. ORIGINATING AGENCY (Corporate and/or)		2a. REPORT SECURITY CLASSIFICATION	
Stanford Electronics Laboratories Stanford University Stanford, California 94305		Unclassified	
2b. GROUP			
3. REPORT TITLE			
THEORY AND PERFORMANCE OF N-PATH FILTERS			
4. DESCRIPTIVE NOTES (Type of report and inclusive dates)			
Technical Report No. 3602-1, May 1971			
5. AUTHOR(S) (First name, middle initial, last name)			
Allston L. Jones			
6. REPORT DATE		7a. TOTAL NO. OF PAGES	7b. NO. OF REFS
May 1971		78	31
8a. CONTRACT OR GRANT NO.		9a. ORIGINATOR'S REPORT NUMBER(S)	
N00014-67-A-0112-0044		SEL-71-026	
b. PROJECT NO		TR No. 3602-1	
c.		9b. OTHER REPORT NO(S) (Any other numbers that may be assigned this report)	
d.			
10. DISTRIBUTION STATEMENT			
This document has been approved for public release and sale; its distribution is unlimited.			
11. SUPPLEMENTARY NOTES		12. SPONSORING MILITARY ACTIVITY	
		Joint Services Electronics Program U. S. Army, Navy, and Air Force	
13. ABSTRACT			
<p>This paper has five major sections. In the first, the periodic time varying network with N-identical paths operating between modulators is examined theoretically by the use of Laplace transforms. The transfer function is derived generally and then expanded for sinusoidal and rectangular modulation. In both cases the low-pass to band-pass characteristic is retained assuming low-pass elements in each path. The next section investigates theoretically, the effects of using other than low-pass elements in the N-paths. The results are such that, if a high-pass, first order all-pass, or a simple band-pass are used in the N-paths the resultant transfer function became a variable attenuator, a notch filter or a pair of adjacent band-pass filters respectively. The third major area is that of switching variations. A more practically oriented configuration is introduced, its transfer function variations are determined and then parallel switching is discussed. In the last sections, the "real world" tolerances and other variations of the components are accounted for in the transfer function of the N-path filter and their effects are noted in five disturbance categories, most serious of which are the variations in the modulating waveforms. Then finally there is a detailed implementation of an N-path filter for use in an IF of an AM/FM receiver which was introduced earlier in the literature. This application makes use of electronic bandwidth and frequency variations.</p>			

14	LINK A		LINK B		LINK C	
	ROLE	WT	ROLE	WT	ROLE	WT
INTRODUCTION OF BACKGROUND ON N-PATH FILTERS						
VARIATIONS OF THE STRUCTURE						
REALIZATION PROBLEMS AND TECHNIQUES						
POTENTIAL APPLICATIONS						

THEORY AND PERFORMANCE OF N-PATH FILTERS

by

Allston L. Jones

May 1971

This document has been approved for public
release and sale; its distribution is unlimited.

Technical Report No. 3602-1

This work was supported wholly by the
Joint Services Electronics Program
(U.S. Army, U.S. Navy, and U.S. Air Force)
under Contract N00014-67-A-0112-0044

 Radioscience Laboratory
 Stanford Electronics Laboratories
Stanford University Stanford, California

PREFACE

This paper has five major sections. In the first, the periodic time varying network with N -identical paths operating between modulators is examined theoretically by the use of Laplace transforms. The transfer function is derived generally and then expanded for sinusoidal and rectangular modulation. In both cases the low-pass to band-pass characteristic is retained assuming low-pass elements in each path. The next section investigates theoretically, the effects of using other than low-pass elements in the N -paths. The results are such that, if a high-pass, first order all-pass, or a simple band-pass are used in the N -paths the resultant transfer function became a variable attenuator, a notch filter or a pair of adjacent band-pass filters respectively. The third major area is that of switching variations. A more practically oriented configuration is introduced, its transfer function variations are determined and then parallel switching is discussed. In the last sections, the "real world" tolerances and other variations of the components are accounted for in the transfer function of the N -path filter and their effects are noted in five disturbance categories, most serious of which are the variations in the modulating waveforms. Then finally there is a detailed implementation of an N -path filter for use in an IF of an AM/FM receiver which was introduced earlier in the literature. This application makes use of electronic bandwidth and frequency variations.

The author wishes to express his gratitude to Professor A. M. Peterson, of the Electrical Engineering Department, Stanford University, for his continued interest, as well as, useful comments and suggestions.

CONTENTS

	<u>Page</u>
I. INTRODUCTION	1
II. TRANSFER FUNCTION DERIVATION	3
A. Sinusoidal Modulation	9
B. Rectangular Modulation	10
III. VARIATIONS OF THE $H(s)$ FUNCTION	17
A. $H(s)$ --Simple High-Pass Filter	21
B. $H(s)$ --First Order All Pass Section	21
C. $H(s)$ --Simple Bandpass Filter	22
D. $H(s)$ --More Complex Functions	25
IV. SWITCHING VARIATIONS	27
A. Shunt Switching Variations	37
V. N-PATH REALIZATION PROBLEM	39
A. Interference Effect	39
B. Discussion of Means to Minimize the Interference Effect	46
C. The Selectivity Problem	48
VI. APPLICATIONS	53
A. Implementation Example	54
VII. CONCLUSIONS	65
Appendix 1. LAPLACE TRANSFORM PAIRS	67
BIBLIOGRAPHY	69

BLANK PAGE

ILLUSTRATIONS

<u>Figure</u>		<u>Page</u>
1.	Block diagram of series multiplier N-path filter	3
2.	Synchronization of multiplier control function	4
3.	Frequency spectrum of $H(j\omega)$ and $H(j\omega \pm j\omega_0)$	9
4.	Rectangular modulated N-path filter damping with various values of N	12
5.	N-path filter response curve with simple RC low pass sections for $H(j\omega)$	14
6.	Pole-zero and loci maps for $H(s) = s/(s+1)$ (high pass)	22
7.	Pole-zero and loci maps for $H(s) = (s-1)/(s+1)$ (all pass)	23
8.	Pole-zero and loci maps for $H(s) = s/(s^2+2s+2)$ (band pass)	24
9.	Series commutated N-path filter with a pair of rotary switches rotating at a frequency of ω_0	27
10.	General notation of switched N-path filter	28
11.	Single path structure for developing the transfer function of the N-path filter with the complete structure as in Fig. 10	28
12.	Insertion attenuation η_N versus N for a series switched N-path filter	34
13.	Harmonic response attenuation with respect to the fundamental frequency for a three section filter	35
14.	Frequency spectrum of a three path switched filter	35
15.	Shunt switched equivalent for Fig. 10	37
16.	Generalization of a single path of an N-path filter showing the voltage notation and including input and output series multipliers	40
17.	Three-path single-ended/push-pull configuration	47
18.	Single path configuration	49

ILLUSTRATIONS (Cont)

<u>Figure</u>		<u>Page</u>
19.	Relative damping and selectivity for a N-path filter . .	51
20.	AM/FM integrated receiver	55
21.	Active second order low-pass filter	56
22.	Active second order 3-path filter	57
23.	s-plane plot of N-path filter poles	59
24.	Third order 3-path filter	61
25.	Bandwidth switching configuration	62
26.	Variable bandwidth characteristic of filter response . .	63

Chapter I

INTRODUCTION

By many, N-path filters are considered to be of rather recent interest, but in fact, papers on this topic appeared as early as 1947. Probably the foremost reason for this general feeling is that this specialized network was, and still is, referred to by no less than eight different names and probably more. Some of these names are: modulated filters [BA1, BA2, DA2, MA1, MA2], comb filters [LE1], commutated filters [BR1, FI1, SM1, SU1, SU2], quadrature function filters [PA1, WE1], sampled-data filters [FR2, LI1], digital filters [HA1, TH1], switched filters [AC1, AC2], and N-path filters [FR1, GL1, GL2, LA1, LA2, LA3, LA4, MO1].

Thus, as can be seen from above, many papers indeed have already been written on some phase of N-path filters. The motivation of this paper is not just to introduce another which discusses a very narrow portion of the subject, but rather, to try to draw together discussions of the theory, the variations, the realization problems and applications of N-path filters.

Why study N-path filters? From experience we have discovered that a low frequency band-pass filter with sharp skirts is very hard to produce using an RLC network or by using active RC techniques. The stability of these networks and the parts tolerances at these low frequencies present economic and challenging technological problems. Also when we consider the need for an inductorless filter for integrated circuits, the N-path filter appears to be very attractive since there are very few other good choices.

The N-path filter is a periodic time varying network which consists of N identical paths, each with a linear time-invariant network, operated, most simply, between a set of input and output modulators. By using a low-pass filter in each of the N-paths, the overall response of the network will be a low-pass to band-pass transformation.

In the earlier sections, the discussions are mainly centered on the theoretical characteristics of this network using low-pass elements in each path. Then, later in the development, other elements are introduced

into each path and the results noted. The more practical nature of the device and the problems that are associated with them begin to come into view at this time. Soon it is learned that a very close match of the transmission characteristics of each path is needed for acceptable performance. This matter is discussed further, two active circuit configurations are introduced in an effort to alleviate the inherent realization problems and a detailed application is cited using the ideas previously introduced.

Chapter II

TRANSFER FUNCTION DERIVATION

Consider the following special arrangement of multipliers, M_{1n} and M_{2n} , the N identical linear time-invariant networks with the impulse response $h(t)$, and the multiplier controlling frequency $f_0 = 1/T$ shown in Fig. 1. The time functions $u_1(t)$ and $u_2(t)$ may

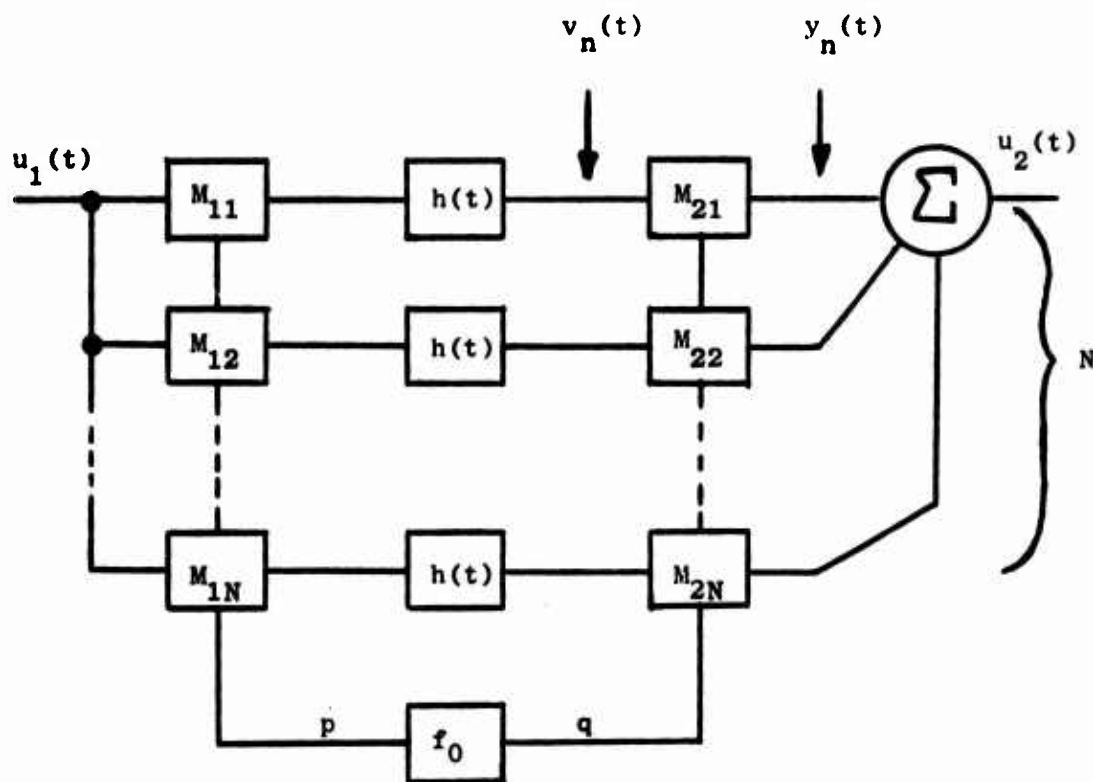


Fig. 1. BLOCK DIAGRAM OF SERIES MULTIPLIER N-PATH FILTER.

be interpreted to be either voltages or currents. Also shown in the block diagram, the multiplier controlling functions $p(t)$ and $q(t)$ are synchronized by f_0 so that both the input and output are advanced without any phase lag. The following discussion is based on those of Langer [LA1], and Franks and Sandberg [FR1].

When, for instance, the multiplier controlling functions $p_n(t)$ and $q_n(t)$ are a series of rectangular impulses, their form is as shown in Fig. 2. The periodic functions $p(t)$ and $q(t)$, in general, can be expressed by their complex Fourier series:

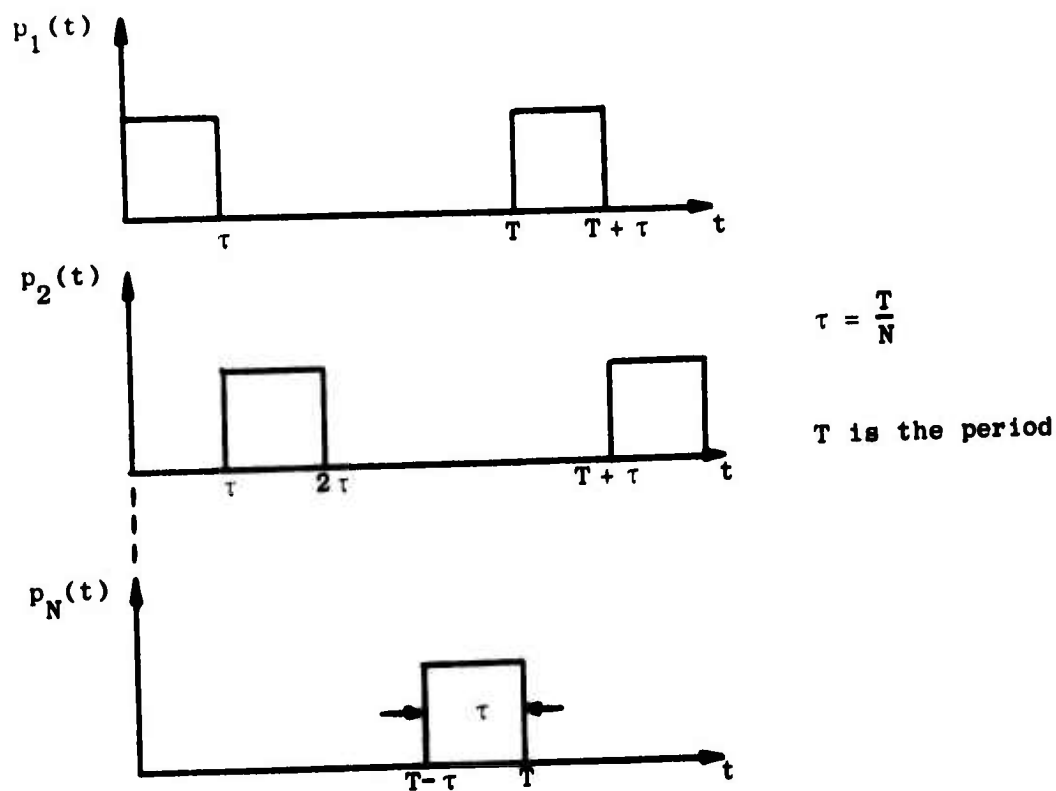


Fig. 2. SYNCHRONIZATION OF MULTIPLIER CONTROL FUNCTION.

$$p(t) = \sum_{\alpha=-\infty}^{+\infty} P_{\alpha} \exp[j\omega_0 \alpha t] \quad (1)$$

$$q(t) = \sum_{\beta=-\infty}^{+\infty} Q_{\beta} \exp[j\omega_0 \beta t]$$

where $\omega_0 = 2\pi/T = 2\pi/N\tau = 2\pi f_0$, and for any specific $p_n(t)$ or $q_n(t)$

$$p_n(t) = p[t - (n - 1) \tau] \quad (2)$$

$$q_n(t) = q[t - (n - 1) \tau]$$

thus yielding

$$p_n(t) = \sum_{\alpha=-\infty}^{\alpha=+\infty} P_{\alpha} \exp\{j\omega_0\alpha[t - (n-1)\tau]\} \quad (3)$$

$$q_n(t) = \sum_{\beta=-\infty}^{\beta=+\infty} Q_{\beta} \exp\{j\omega_0\beta[t - (n-1)\tau]\}$$

P_{α} and Q_{β} are the Fourier coefficients of $p_n(t)$ and $q_n(t)$, and they are fixed by the type of waveform which $p_n(t)$ and $q_n(t)$ are; e.g., sine, rectangular pulse, etc.

The output $u_2(t)$ of the network shown in Fig. 1 is composed of the functions $p_n(t)$, $q_n(t)$, $h(t)$, and the input $u_1(t)$ summed over all N channels. Since multiplication in the time domain corresponds to convolution in the frequency domain, it follows that

$$u_2(t) = \sum_{n=1}^N y_n(t) = \sum_{n=1}^N q_n(t) \{h(t) * [p_n(t)u_1(t)]\} = \sum_{n=1}^N v_n(t) q_n(t) \quad (4)$$

where

$$v_n(t) = h(t) * [u_1(t)p_n(t)]$$

Converting to the frequency domain by means of the Laplace transformation

$$U_2(s) = \sum_{n=1}^N V_n(s) * Q_n(s) \quad (5)$$

If $h(t)$ is not only passive, but also time invariant and has constant parameters, it follows that

$$V_n(s) = [U_1(s) * P_n(s)] H(s) \quad (6)$$

In order to evaluate Eq. (6), $P_n(s)$ must be determined. Thus from Eq. (3)

$$p_n(t) = \sum_{\alpha} P_{\alpha} \exp[j\omega_0 \alpha t] \exp[-j\omega_0 \alpha (n-1) \tau] \quad (7)$$

and applying the Laplace transformation

$$P_n(s) = \sum_{\alpha} P_{\alpha} \exp[-j\omega_0 \alpha (n-1) \tau] \cdot \frac{1}{s - j\omega_0 \alpha} \quad (8)$$

since $\mathcal{L}\{\exp[at]\} = 1/(s-a)$.

Using the results of Eq. (8) and

$$F(s) * \frac{1}{s-a} = F(s-a) \quad (9)$$

the following is obtained

$$U_1(s) * P_n(s) = \sum_{\alpha} P_{\alpha} \exp[-j\omega_0 \alpha (n-1) \tau] U_1(s - j\omega_0 \alpha) \quad (10)$$

Thus, by combining Eqs. (6) and (10), it follows that

$$V_n(s) = \sum_{\alpha} P_{\alpha} \exp[-j\omega_0 \alpha (n-1) \tau] U_1(s - j\omega_0 \alpha) H(s) \quad (11)$$

By combining Eqs. (5) and (11), and by again applying Eq. (9), it can be shown that

$$V_2(s) = \sum_n \sum_{\alpha} \sum_{\beta} P_{\alpha} Q_{\beta} \exp[-j\omega_0 (\alpha + \beta) (n-1) \tau] U_1[s - j\omega_0 (\alpha + \beta)] H(s - j\omega_0 \beta) \quad (12)$$

The summation over n is a geometric series with the quotient

$$q = \exp[-j\omega_0(\alpha + \beta)\tau] \quad (13)$$

The summation over n can be written as

$$\sum_{n=1}^N \exp[-j\omega_0(n-1)(\alpha + \beta)\tau] = \frac{q^N - 1}{q - 1} = \frac{\exp[-j\omega_0(\alpha + \beta)\tau N] - 1}{\exp[-j\omega_0(\alpha + \beta)\tau] - 1} \quad (14)$$

Since $\omega_0 = 2\pi/T$ and $\tau = T/N$, the sum becomes

$$\sum_n \exp[-j\omega_0(n-1)(\alpha + \beta)\tau] = \frac{\exp[-j2\pi(\alpha + \beta)] - 1}{\exp[-j2\pi(\alpha + \beta)/N] - 1} \quad (15)$$

for $\alpha + \beta = \text{integer}$. When $(\alpha + \beta)/N = \text{integer}$ also, the term is an indeterminate form of the type $0/0$. The limit of the fraction

$$\lim_{\frac{\alpha + \beta}{N} \rightarrow k} \frac{\exp[-j2\pi(\alpha + \beta)] - 1}{\exp[-j2\pi(\alpha + \beta)/N] - 1} = \lim_{\frac{\alpha + \beta}{N} \rightarrow k} \frac{N \exp[-j2\pi(\alpha + \beta)]}{\exp[-j2\pi(\alpha + \beta)/N]} = N \quad (16)$$

by applying l'Hospital's rule. The above is true only when α , β and k are integers (positive or negative) and N is a positive integer.

Thus

$$\sum_{n=1}^N \exp[-j\omega_0(\alpha + \beta)(n-1)\tau] = N, \quad \text{for } \alpha + \beta = kN \quad (17)$$

$$= 0, \quad \text{otherwise}$$

Now, by combining Eqs. (12) and (17), $U_2(s)$ is obtained

$$U_2(s) = N \sum_{\alpha} \sum_{\beta} P_{\alpha} Q_{\beta} U_1[s - j\omega_0(\alpha + \beta)] H(s - j\omega_0\beta) \quad \text{for } \alpha + \beta = kN \quad (18)$$

If we let $\alpha = kN - \beta$, then Eq. (18) becomes

$$U_2(s) = N \sum_{\beta} \sum_k P_{kN-\beta} Q_{\beta} U_1[s - j\omega_0 kN] H(s - j\omega_0 \beta) \quad (19)$$

From Eq. (19) it can be seen that the summation over the two independent indices β and k yields a spectrum of u_2 with infinitely many overlapping terms.

By imposing certain band limiting restrictions on the input signals, a transfer function relation between input and output can be derived. By introducing a low-pass filter in series with the input, such that, $U_1(s)$ evaluated on the $j\omega$ -axis essentially vanishes outside the interval $|\omega| < N\omega_0/2$. The $U_1[s - j\omega_0 kN]$ term, from Eq. (19), satisfies the restriction $|\omega| < N\omega_0/2$ only when $\omega_0 kN < N\omega_0/2$, and this only holds when $k = 0$. Thus

$$U_2(s) = N \sum_{\beta} P_{-\beta} Q_{\beta} U_1(s) H(s - j\omega_0 \beta) \quad (20)$$

By examining the above equation, it can be seen that it represents a low-pass to band-pass transformation with all the harmonics and a dc component if the $H(j\omega)$ represents a low-pass filter. Therefore, if ω_0 is considered to be the center frequency, β becomes the harmonic index ($\omega_I \geq \omega_0/2$, $\omega_{II} \leq 3\omega_0/2$ being the lower and upper cut-off frequencies). Thus, selecting $\beta = \pm 1$ making ω_0 the center frequency:

$$G(s) = \frac{U_2(s)}{U_1(s)} = N \left[P_{-1} Q_1 H(s - j\omega_0) + P_1 Q_{-1} H(s + j\omega_0) \right] \quad (21)$$

the impulse response for the low pass-bandpass transformation.

As has been noted above, the center frequency of the bandpass response is determined by the frequency of the modulation of the paths. The half-power frequency, on the other hand, is determined by the cut-off frequency of the N identical low pass filters in the N paths (see Fig. 3).

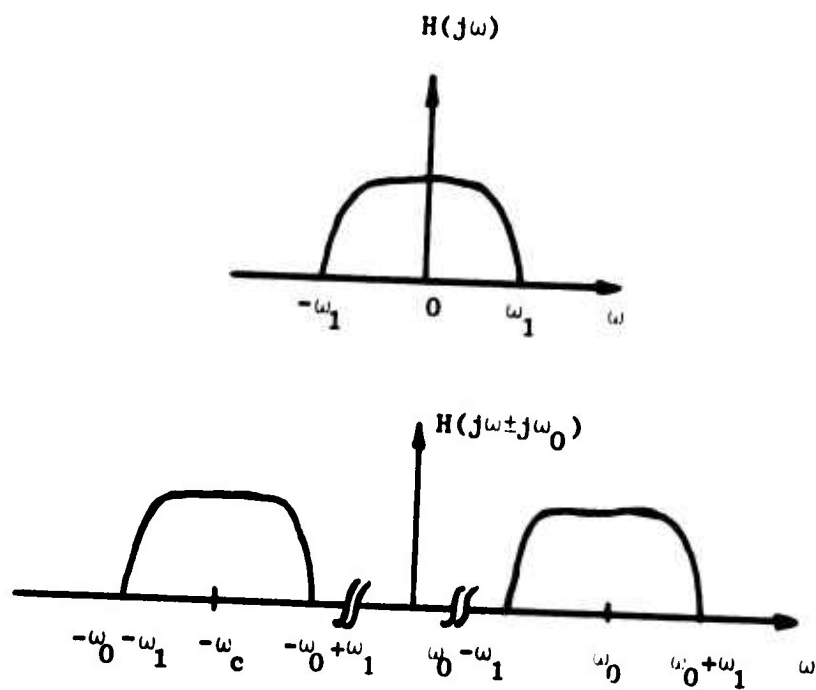


Fig. 3. FREQUENCY SPECTRUM OF $H(j\omega)$ AND $H(j\omega \pm j\omega_0)$.

Of particular importance to the circuit's ability to hold the center frequency ω_0 is the tolerance and instability of all the independent network components. As yet, it has not been shown what effect the modulation voltage waveform and path number have on the transfer function $G(s)$.

Two modulating functions of particular interest; the sine wave, and the rectangular wave with amplitude will be discussed next.

A. Sinusoidal Modulation

The coefficients of the complex Fourier series for

$$P_n(t) = q_n(t) = A \sin \omega_0 t \quad (22)$$

where A is the amplitude, are

$$P_{\alpha} = Q_{\alpha} = \frac{1}{T} \int_0^T A \sin \omega_0 t \exp[-j\omega_0 \alpha t] = \begin{cases} \frac{-j}{2} A & \text{for } \alpha = +1 \\ \frac{j}{2} A & \text{for } \alpha = -1 \\ 0 & \text{for } \alpha \neq \pm 1 \end{cases} \quad (23)$$

thus

$$P_{kN-\beta} Q_{\beta} \equiv 0 \quad \text{for } k \neq 0 \quad \text{and } N > 2\beta \quad (24)$$

The transfer function using the above results on Eq. (21), is

$$G(s) = \frac{U_2(s)}{U_1(s)} = N \left[\frac{A^2}{4} H(s - j\omega_0) + \frac{A^2}{4} H(s + j\omega_0) \right] \quad \text{for } N > 2 \quad (25)$$

Equation (25) shows that for sinusoidal modulation the transfer function is real, and directly proportional to the number of paths and the square of the magnitude of the sinusoidal modulating function. With the $N > 2\beta$ restriction, the transfer function $G(s)$ is true without further band-limiting restrictions.

B. Rectangular Modulation

This method of modulating the filter is of particular practical importance since the modulation may alternately be implemented by simple transistor switching. The switching frequency would still be $\omega_0 = 2\pi/T$ and the switching time would be $\tau = T/N$ where τ is the on or dwell time of each path.

The switching or gating time function is

$$p_n(t) = \begin{cases} 1 & \text{for } (n-1)\tau + (v-1)T \leq t \leq n\tau + (v-1)T \\ 0 & \text{for all other } t \end{cases} \quad \nu = 1, 2, 3, \dots \quad (26)$$

and $q_n(t)$ is analogous to $p_n(t)$.

The derivation of the Fourier coefficients P_α and Q_β are of the form

$$\begin{aligned}
 P_\alpha &= \frac{1}{T} \int_0^T p(t) \exp[-j\omega_0 \alpha t] dt \\
 &= \frac{1}{T} \int_0^T \exp\left[-j \cdot \frac{2\pi}{T} \alpha t\right] dt \\
 &= \frac{j}{2\pi\alpha} \left[\exp\left(-j \cdot \frac{2\pi\alpha}{T} \tau\right) - 1 \right] \\
 &= \frac{j}{2\pi\alpha} \left[\exp\left(-j \cdot \frac{2\pi\alpha}{N}\right) - 1 \right] = \frac{j}{2\pi\alpha} \exp\left(-j \cdot \frac{\pi\alpha}{N}\right) \left[\exp\left(-j \cdot \frac{\pi\alpha}{N}\right) - \exp\left(j \cdot \frac{\pi\alpha}{N}\right) \right] \\
 &= \exp\left[-j \cdot \frac{\pi\alpha}{N}\right] \cdot \frac{\sin \frac{\pi\alpha}{N}}{\pi\alpha}
 \end{aligned} \tag{27}$$

Similarly

$$Q_\beta = \exp\left[-j \cdot \frac{\beta\pi}{N}\right] \cdot \frac{\sin \frac{\beta\pi}{N}}{\beta\pi} \tag{28}$$

Thus

$$P_{-1}Q_1 = \frac{\sin^2 \frac{\pi}{N}}{\pi^2} \quad \text{and} \quad P_1Q_{-1} = \frac{\sin^2 \frac{\pi}{N}}{\pi^2} \tag{29}$$

Substituting these results into Eq. (21) yields

$$G(s) = \frac{U_2(s)}{U_1(s)} = N \frac{\sin^2 \frac{\pi}{N}}{\pi^2} \left[H(s - j\omega_0) + H(s + j\omega_0) \right] \tag{30}$$

The network damping function is dependent on N and can be considered to be the insertion attenuation of the filter

$$\gamma_N = N \frac{\sin^2 \frac{\pi}{N}}{\pi^2} \quad (31)$$

where for $N = 2$

$$\gamma_2 = \frac{2}{\pi^2}$$

and for $N = 3$

$$\gamma_3 = \frac{9}{4\pi^2}$$

and ultimately

$$\lim_{N \rightarrow \infty} \gamma_N = 0$$

Thus the maximum output occurs when $N = 3$ (see Fig. 4). This is not a strict requirement for the minimum number of paths being $N = 3$.

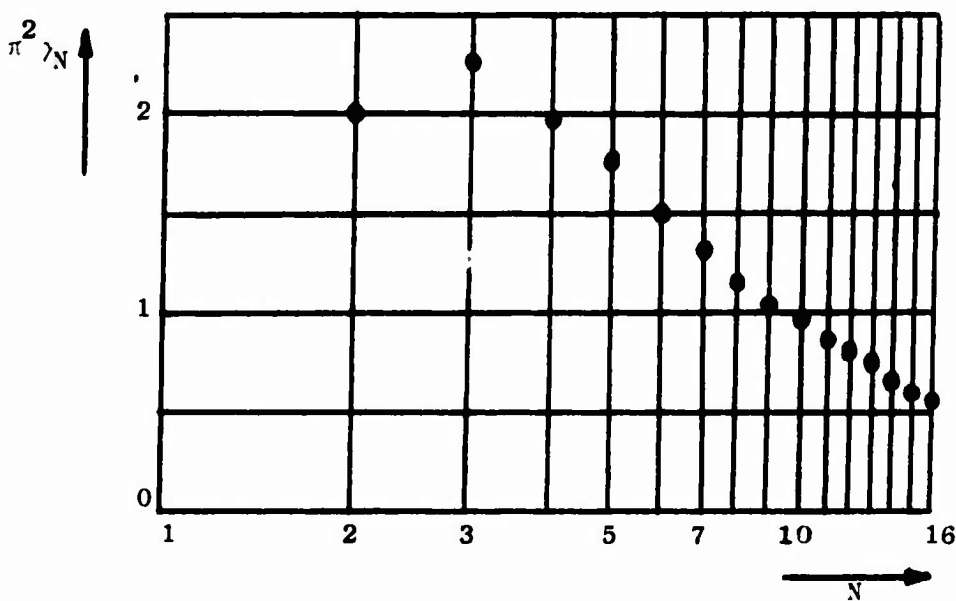


Fig. 4. RECTANGULAR MODULATED N-PATH FILTER DAMPING WITH VARIOUS VALUES OF N .

Then, in order to avoid the multivalued and overlapping terms in Eq. (20), we put the restriction on the input $U_1(s)$ that $|\omega| \leq N\omega_0/2$ thus necessitating $N \geq 3$.

To illustrate the fact that the bandwidth of the N-path filter is due strictly to the bandwidth of the $H(j\omega)$ function and is independent of the center frequency ω_0 , consider a simple low-pass RC network such that the low pass-bandpass transformation maps $H(j\omega)$ into $H(j\omega - j\omega_0)$. To make the synthesis of a filter with a center frequency in the MHz range possible, it is necessary to have a very stable switching frequency ω_0 . Assume that the real portion of the frequency function $s = a + j\omega$ is zero, such that $s = j\omega$, then:

$$G(s) \rightarrow G(j\omega)$$

From Eq. (30)

$$G(j\omega) = \frac{U_2(j\omega)}{U_1(j\omega)} = N \frac{\sin^2 \frac{\pi}{N}}{\pi^2} \left[H(j\omega - j\omega_0) + H(j\omega + j\omega_0) \right] \quad (32)$$

From the right term in the above it can be seen that the response is a mirror image around the frequency ω_0 .

Let

$$H(j\omega) = \frac{1}{1 + j\omega RC} \quad (33)$$

which is a single low pass section with the cut-off frequency ω_g ,

$$\omega_g = \frac{1}{RC} \quad (34)$$

so that

$$|H(j\omega)| = \left| \frac{1}{1 + j\omega RC} \right| = \frac{\pm 1}{\sqrt{\omega^2 R^2 C^2 + 1}} = \frac{\pm 1}{\sqrt{\left(\frac{\omega}{\omega_g}\right)^2 + 1}} \quad (35)$$

and

$$|H(j\omega - j\omega_0)| = \frac{\pm 1}{\sqrt{(\omega - \omega_0)^2 R^2 C^2 + 1}} = \frac{\pm 1}{\sqrt{\left(\frac{\omega - \omega_0}{\omega_g}\right)^2 + 1}} \quad (36)$$

Assuming that

$$f_0 = 1 \text{ MHz}$$

$$f_g = 1 \text{ kHz}$$

then using Eq. (36) the response curve $|H(j\omega - j\omega_0)|$ can be plotted as shown in Fig. 5. From this curve it can be observed that the response is strictly symmetric around f_0 . It may also be noted that this is the response of a simple LC bandpass filter.

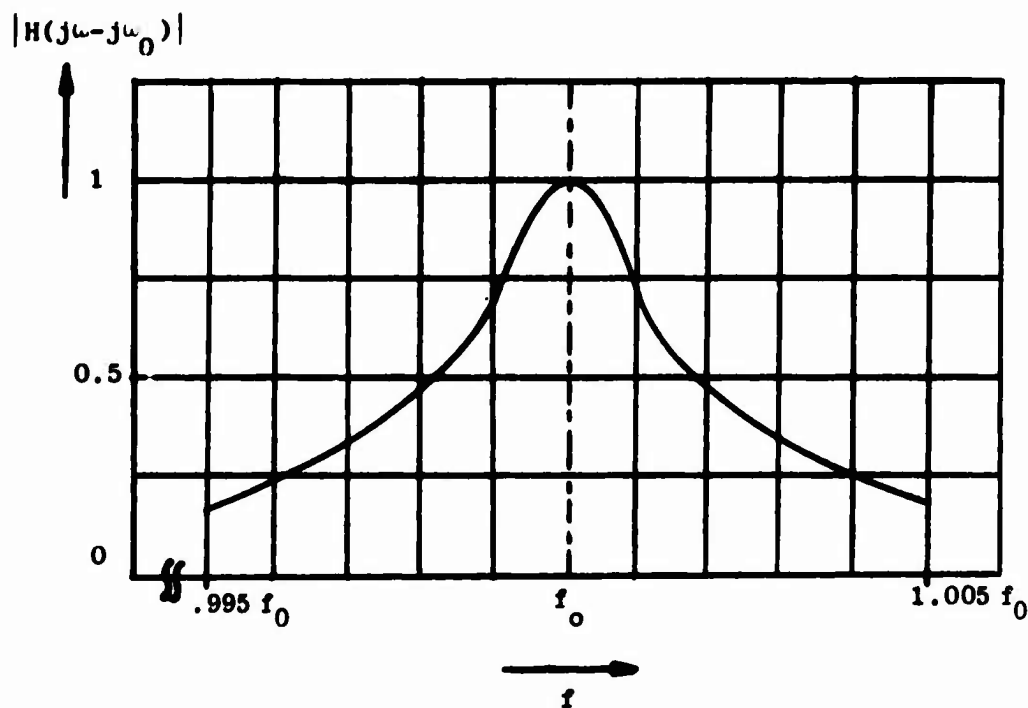


Fig. 5. N-PATH FILTER RESPONSE CURVE WITH SIMPLE RC LOW PASS SECTIONS FOR $H(j\omega)$.

From Fig. 5, observe that the 3 db bandwidth is 2 kHz, since it was assumed that $f_0 = 1$ MHz. From the well known relation that

$$Q = \frac{f_0}{BW} \quad (37)$$

this arrangement theoretically would have a Q of 500.

Considering the $H(j\omega)$ function to be strictly that of a low-pass filter, and if the cut-off frequency of that low-pass filter is to be sufficiently low, i.e.,

$$\omega_g \leq N \frac{\omega_0}{2} \quad (38)$$

then the input filter on the N-path filter, considered in the paragraph just above, Eq. (20) becomes unnecessary. That is to say, that the condition on the input established at that time, is replaced by $H(j\omega)$ being a low-pass filter that satisfies the condition of Eq. (38). If Eq. (38) is rearranged and the result substituted into Eq. (37), a very interesting result is obtained, i.e.,

$$\omega_0 \geq \frac{2\omega_g}{N} \quad \text{or} \quad f_0 \geq \frac{2f_g}{N}$$

thus

$$Q = \frac{f_0}{BW} \geq \frac{2f_g}{NBW} \quad (39)$$

A broadband filter on the output of the N-path filter is also necessary to recover the single "tuned" bandwidth of interest, if a "comb filter" response is not desired.

BLANK PAGE

Chapter III

VARIATIONS OF THE $H(s)$ FUNCTION

The previous section was only concerned with $H(s)$ being a low-pass filter since the transfer function $G(s)$ represented the standard low-pass-bandpass transformation. Here, a discussion of the form of $G(s)$ when $H(s)$ represents other than a low pass structure is presented as developed by Acampora [AC2].

Observing Eqs. (25) and (30), it can be seen that a basic generalization of the transfer function is possible, i.e.,

$$G(s) = \frac{U_2(s)}{U_1(s)} = K \left[H(s - j\omega_0) + H(s + j\omega_0) \right] \quad (40)$$

Assuming that $H(s)$ can be written as a ratio of two finite degree polynomials $N(s)$ (unrelated to the constant N used in Chapter II) and $D(s)$, then

$$\begin{aligned} G(s) &= K \left[\frac{N(s - j\omega_0)}{D(s - j\omega_0)} + \frac{N(s + j\omega_0)}{D(s + j\omega_0)} \right] \\ &= K \left[\frac{N(s - j\omega_0)D(s + j\omega_0) + N(s + j\omega_0)D(s - j\omega_0)}{D(s - j\omega_0)D(s + j\omega_0)} \right] \quad (41) \\ &= K \frac{P(s)}{Q(s)} \end{aligned}$$

The poles of $G(s)$ are dependent only on the poles of $H(s)$; the zeros of $G(s)$ are not as simple.

The following develops a more general expression for the numerator of $G(s)$. Using the Laplace transform-pair correspondence [see Appendix, Eq. (A.1)], the numerator products can be written as convolved time domain functions, as follows:

$$P(s) \leftrightarrow \int_{-\infty}^{+\infty} \left\{ d(\tau) \left[\exp(-j\omega_0 \tau) \right] n(t - \tau) \left[\exp(j\omega_0 (t - \tau)) \right] \right. \\ \left. + d(\tau) \left[\exp(j\omega_0 \tau) \right] n(t - \tau) \left[\exp(-j\omega_0 (t - \tau)) \right] \right\} d\tau \quad (42)$$

or

$$P(s) \leftrightarrow \int_{-\infty}^{+\infty} d(\tau) n(t - \tau) \left[\exp(j\omega_0 (t - 2\tau)) + \exp(-j\omega_0 (t - 2\tau)) \right] d\tau \quad (43)$$

$$P(s) \leftrightarrow 2 \int_{-\infty}^{+\infty} d(\tau) n(t - \tau) \cos \omega_0 (t - 2\tau) d\tau \quad (44)$$

Expanding $\cos x$ as

$$\cos x = 1 - \frac{x^2}{2!} + \frac{x^4}{4!} - \dots \quad (45)$$

Thus

$$P(s) \leftrightarrow 2 \int_{-\infty}^{+\infty} d(\tau) n(t - \tau) \left[1 - \frac{\omega_0^2 (t - 2\tau)^2}{2!} + \frac{\omega_0^4 (t - 2\tau)^4}{4!} + \dots \right. \\ \left. + \frac{(-1)^k \left[\omega_0 (t - 2\tau)^{2k} \right]}{(2k)!} + \dots \right] d\tau \quad (46)$$

Rewriting

$$P(s) \leftrightarrow 2 \int_{-\infty}^{+\infty} d(\tau) n(t - \tau) \left[1 - \frac{\omega_0^2}{2!} \left[(t - \tau) - \tau \right]^2 + \frac{\omega_0^4}{4!} \left[(t - \tau) - \tau \right]^4 + \dots \right. \\ \left. + \frac{(-1)^k \omega_0^{2k}}{(2k)!} \left[(t - \tau) - \tau \right]^{2k} + \dots \right] d\tau \quad (47)$$

and

$$\begin{aligned}
 P(s) \leftrightarrow 2 \left\{ \int_{-\infty}^{+\infty} d(\tau)n(t-\tau)d\tau - \frac{\omega_0^2}{2!} \int_{-\infty}^{+\infty} d(\tau)n(t-\tau) \left[(t-\tau)^2 - 2(t-\tau)\tau \right. \right. \\
 \left. \left. + (t-\tau)\tau^2 \right] d\tau + \dots + \frac{(-1)^k \omega_0^{2k}}{(2k)!} \int_{-\infty}^{+\infty} d(\tau)n(t-\tau) \left[(t-\tau)^{2k} \right. \right. \\
 \left. \left. - 2k(t-\tau)^{2k-1}\tau + \frac{2k(2k-1)}{2!} (t-\tau)^{2k-2}\tau^2 + \dots + \tau^{2k} \right] d\tau + \dots \right\} \quad (48)
 \end{aligned}$$

using the binomial theorem of expansion. Or, finally,

$$\begin{aligned}
 P(s) = 2 \left\{ N^0(s)D^0(s) - \frac{\omega_0^2}{2!} \left[N^2(s)D^0(s) - 2N^1(s)D^1(s) + N^0(s)D^2(s) \right] \right. \\
 + \frac{\omega_0^4}{4!} \left[N^4(s)D^0(s) - 4N^3(s)D^1(s) + 6N^2(s)D^2(s) \right. \\
 \left. - 4N^1(s)D^3(s) + N^0(s)D^4(s) \right] + \dots \\
 + \frac{(-1)^k \omega_0^{2k}}{(2k)!} \left[N^{2k}(s)D^0(s) - 2kN^{2k-1}(s)D^1(s) \right. \\
 \left. + \frac{2k(2k-1)}{2!} N^{2k-2}(s)D^2(s) + \dots + N^0(s)D^{2k}(s) \right] + \dots \left. \right\} \quad (49)
 \end{aligned}$$

where the superscripts on the $N(s)$ and $D(s)$ functions denote derivatives with respect to s . $P(s)$ may be rewritten in the following shorthand notation:

$$P(s) = 2 \left\{ T_0(s) + \omega_0^2 T_1(s) + \omega_0^4 T_2(s) + \dots + \omega_0^{2k} T_k(s) + \dots \right\} \quad (50)$$

where

$$T_0(s) = N^0(s)D^0(s)$$

$$T_1(s) = \frac{-1}{2!} \left[N^2(s)D^0(s) - 2N^1(s)D^1(s) + N^0(s)D^2(s) \right] \quad (51)$$

$$T_k(s) = \frac{(-1)^k}{(2k)!} \left[N^{2k}(s)D^0(s) - 2kN^{2k-1}(s)D^1(s) + \dots + N^0(s)D^{2k}(s) \right]$$

Equation (50) is the generalized form of $P(s)$ that was sought for Eq. (41). It should also be noted that when both $N(s)$ and $D(s)$ are finite degree polynomials, Eq. (50) is truncated at a point where all higher order derivatives of $N(s)$ and $D(s)$ are zero. Letting the degrees of $N(s)$ and $D(s)$ be ℓ and m respectively, then, k , the subscript of the last $T(s)$ function in Eq. (50), is

$$k = \begin{cases} \frac{\ell + m}{2} & \text{if } \ell + m \text{ is even} \\ \frac{\ell + m - 1}{2} & \text{if } \ell + m \text{ is odd} \end{cases} \quad (52)$$

To illustrate the effect of various $h(t)$ functions, it is sufficient to consider the $k = 1$ case. Thus, the transfer function $G(s)$ reduces to:

$$\begin{aligned} G(s) &= 2K \frac{T_0(s) + \omega_0^2 T_1(s)}{D(s - j\omega_0)D(s + j\omega_0)} \\ &= 2K \frac{N(s)D(s) - \frac{\omega_0^2}{2} \left[N^2(s)D^0(s) - 2N^1(s)D^1(s) + N^0D^2(s) \right]}{D(s - j\omega_0)D(s + j\omega_0)} \end{aligned} \quad (53)$$

By examining the above equation, it can be seen that the poles originate at $\omega_0 = 0$ as double roots of $D(s)$ and migrate in straight lines in the $\pm j\omega_0$ directions as direct functions of ω_0 ; however, the zeros originate at the combined roots of $N(s)D(s)$ at $\omega_0 = 0$ and migrate along calculable loci as a function of ω_0 , and the roots finally terminate at the roots of $T_1(s)$ as ω_0 approaches infinity. In the following examples, the established root-locus techniques, as presented by Truxal [TR1] and others, are utilized.

A. H(s)--Simple High-Pass Filter

For this illustration, consider $H(s) = s/(s+1)$, a simple normalized high-pass filter. For this choice of $H(s)$, $N^2(s)D^0(s) = N^0(s)D^2(s) = 0$ and $-2N^1(s)D^1(s) = -2$. Thus

$$G(s) = 2K \frac{s(s+1) + \omega_0^2}{(s+1-j\omega_0)(s+1+j\omega_0)} = K^1 \frac{P(s)}{Q(s)} \quad (54)$$

In Fig. 6, the plots of the roots of $H(s)$ and $G(s)$ are plotted, as well as, the root loci of the poles and zeros of $G(s)$. From these plots and Eq. (54) it can be seen that a commutated high-pass filter leads to a variable attenuator. For the specific $H(s)$ chosen here, the maximum attenuation is 6 db when the poles and zeros of $G(s)$ are nearly horizontally aligned.

B. H(s)--First Order All Pass Section

For the simple all pass section consider $H(s) = (s-1)/(s+1)$. Again, $N^2(s)D^0(s) = N^0(s)D^2(s) = 0$, and $-2N^1(s)D^1(s) = -2$, such that

$$G(s) = \frac{(s-1)(s+1) + \omega_0^2}{(s+1-j\omega_0)(s+1+j\omega_0)} = \frac{P(s)}{Q(s)} \quad (55)$$

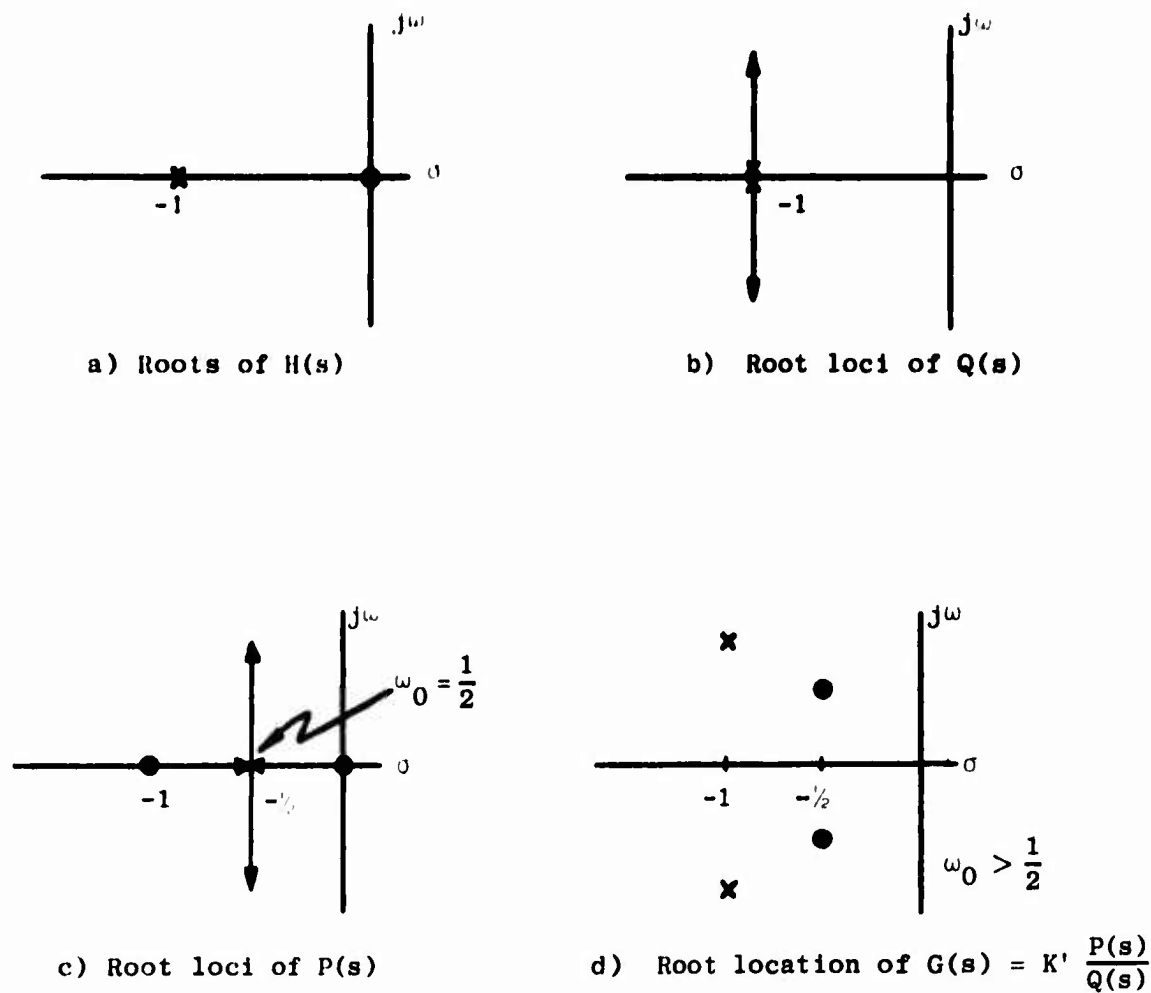


Fig. 6. POLE-ZERO AND LOCI MAPS FOR $H(s) = s/(s+1)$ (HIGH PASS).

The roots of $H(s)$ and $G(s)$, and the root loci of the poles and zeros of $G(s)$ are plotted in Fig. 7. From Fig. 7d it is observed that the first order all pass, when commutated, yields a notch filter.

C. H(s)--Simple Bandpass Filter

Consider next $H(s) = s/(s^2 + 2s + 2)$ for the simple bandpass filter. Thus, $N^2(s)D^0(s) = 0$, $-2N^1(s)D^1(s) = -4s - 4$, $N^0(s)D^2(s) = 2s$; so that

$$G(s) = \frac{s(s^2 + 2s + 2) + \omega_0^2(s + 2)}{D(s - j\omega_0)D(s + j\omega_0)} = \frac{P(s)}{Q(s)}$$

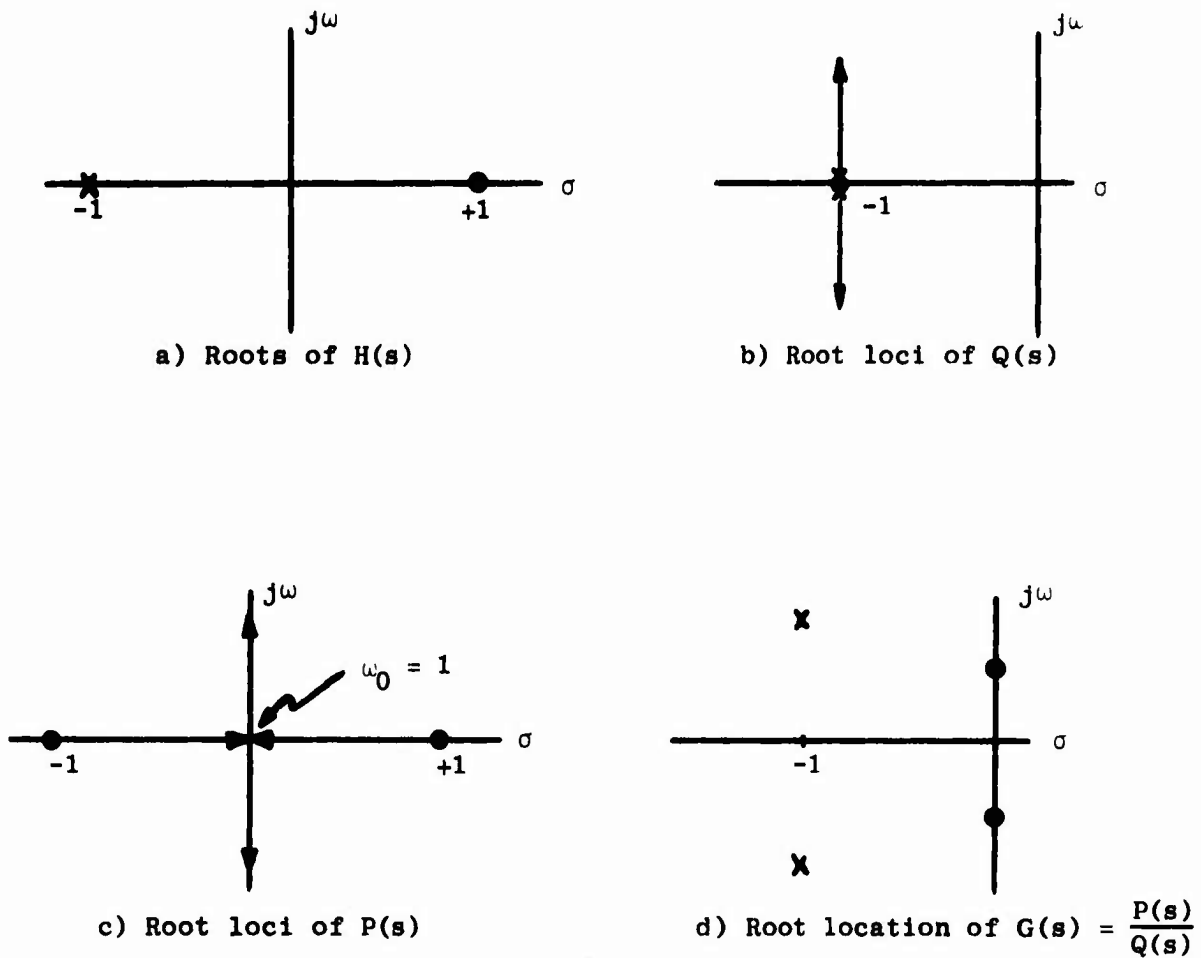
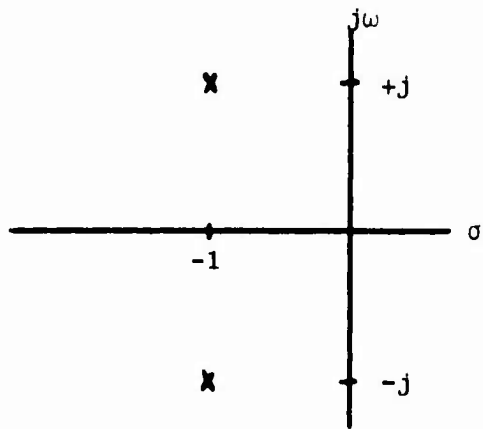
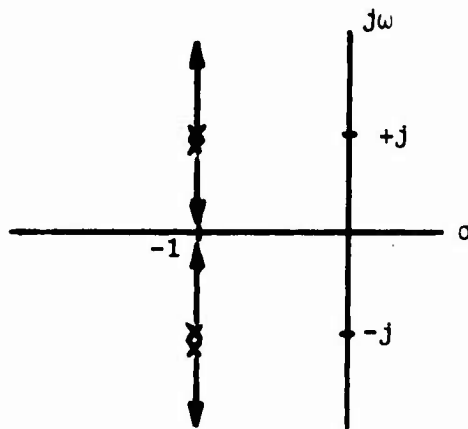


Fig. 7. POLE-ZERO AND LOCI MAPS FOR $H(s) = (s-1)/(s+1)$ (ALL PASS).

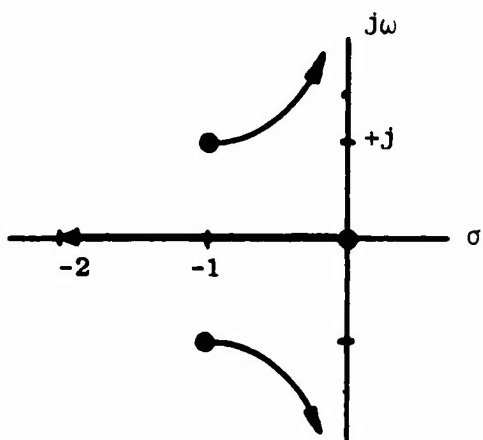
The root loci and the pole-zero patterns are plotted and they are shown in Fig. 8 for this example. Figure 8d reveals that when a simple band-pass filter is commutated, the result is a pair of adjacent bandpass filters with a notch between them that deepens as ω_0 increases and the complex zeros approach the $j\omega$ axis.



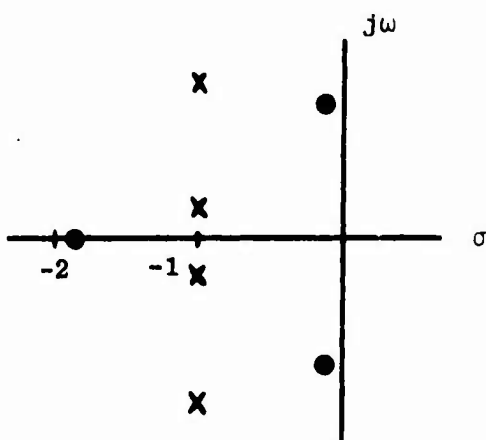
a) Roots of $H(s)$



b) Root loci of $Q(s)$



c) Root loci of $P(s)$



d) Root location of $G(s) = \frac{P(s)}{Q(s)}$

Fig. 8. POLE-ZERO AND LOCI MAPS FOR $H(s) = s/(s^2 + 2s + 2)$ (BAND PASS).

D. H(s)--More Complex Functions

For the simple functions above it was not necessary to develop Eq. (50), instead Eq. (41) could have been used directly. For generalization to more complex transfer functions, Eq. (50) was generated, since the root loci of the zeros of $G(s)$ begin at the roots of $T_0(s)$ and migrate through the roots of $T_1(s), \dots, T_k(s)$; i.e., the roots of $T_n(s)$ roughly terminate at the roots of $T_{n+1}(s)$ for the lower values of k , as k advances this simplicity is also lost.

BLANK PAGE

Chapter IV

SWITCHING VARIATIONS

In the general system block diagram, shown in Fig. 1, the "commutation" of the filter was implemented by the use of series modulators in each leg of the filter, one on the input and another one on the output. For the discussion in Chapter II, where an analog (sinusoid) and a digital (rectangular) form of "commutation" were to be introduced, the modulators provided a technique that could include both types of "commutation." More specifically, since the thrust in recent years has been miniaturization and integration, the potential of the digital "commutation" technique is of particular importance since the digital techniques lend themselves very well to integration.

By using a rectangular or digital form of commutation, the modulators can be replaced by mechanical or electronic commutators on the input and output of the filter. In some of the earliest papers on N-path filters, the filter model included mechanical wafer switches (break before make type) on the input and output (see Fig. 9), thus introducing the terminology of a "commutated filter" [LE1, FI1, SU1].

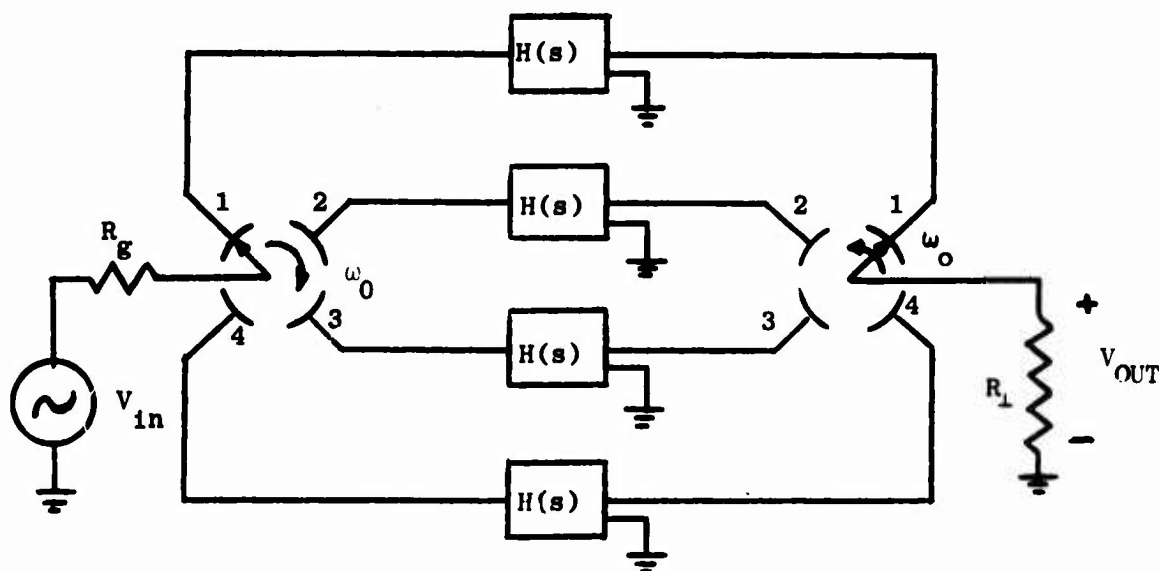


Fig. 9. SERIES COMMUTATED N-PATH FILTER WITH A PAIR OF ROTARY SWITCHES ROTATING AT A FREQUENCY OF ω_0 .

Now consider the configuration shown in Fig. 10 and develop the transfer function for this case, as was done for the rectangular modulation case in Chapter II. The first thing to be realized in this case is that all the resistances for the low pass RC's are lumped together as R_1 preceding the input switches. The individual path network $H(s)$ becomes a shunt reactive network (in Fig. 10 it is shown as a single capacitor). To develop the equations, it is necessary to examine the structure of a single path of the N-path filter as shown in Fig. 11.

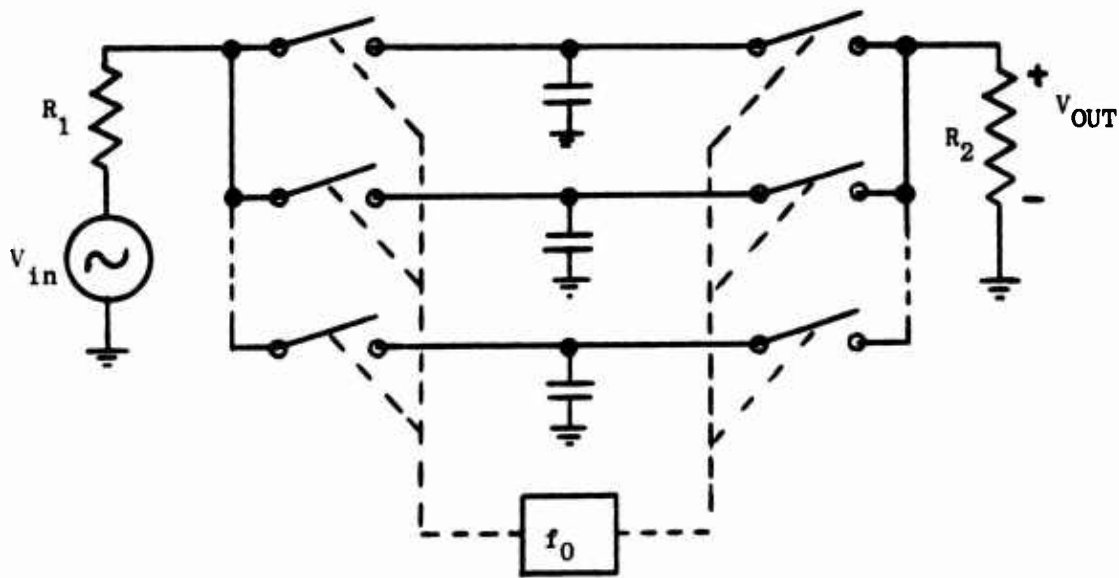


Fig. 10. GENERAL NOTATION OF SWITCHED N-PATH FILTER.

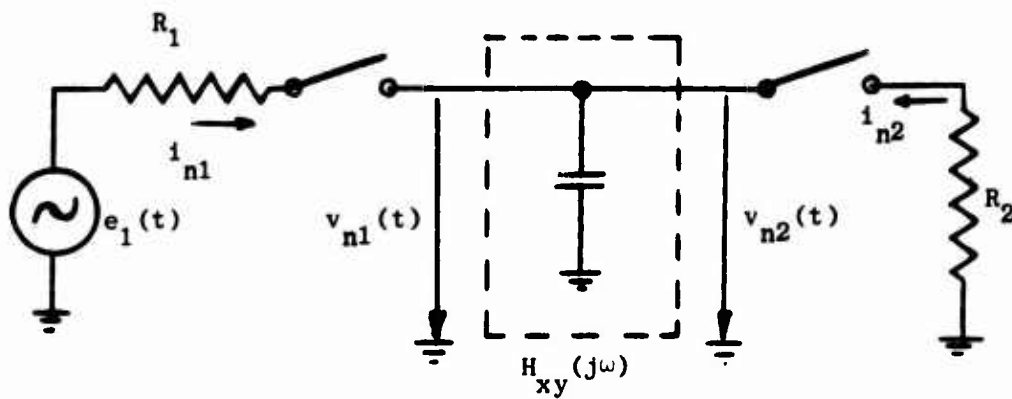


Fig. 11. SINGLE PATH STRUCTURE FOR DEVELOPING THE TRANSFER FUNCTION OF THE N-PATH FILTER WITH THE COMPLETE STRUCTURE AS IN FIG. 10.

The $H_{xy}(j\omega)$ in the figure is the transfer function of the capacitor, such that

$$V_{n1}(j\omega) = H_{11}(j\omega)I_{n1}(j\omega) + H_{12}(j\omega)I_{n2}(j\omega) \quad (56)$$

$$V_{n2}(j\omega) = H_{21}(j\omega)I_{n1}(j\omega) + H_{22}(j\omega)I_{n2}(j\omega)$$

Also from Fig. 11

$$i_{n1} = \frac{e_1(t) - v_{n1}(t)}{R_1} p_n(t) \quad (57)$$

$$i_{n2} = \frac{-v_{n2}(t)}{R_2} q_n(t)$$

where $p_n(t)$ and $q_n(t)$ are the characteristics of the input and output switches respectively. By applying Laplace transform methods

$$I_{n1} = \frac{1}{R_1} \sum_{\alpha=-\infty}^{+\infty} P_{\alpha} \exp\left[-j\omega_0\alpha(n-1) \frac{T}{N}\right] \times \left[E_1(j\omega - j\omega_0\alpha) - V_{n1}(j\omega - j\omega_0\alpha) \right] \quad (58)$$

$$I_{n2} = \frac{-1}{R_2} \sum_{\beta=-\infty}^{+\infty} Q_{\beta} \exp\left[-j\omega_0\beta(n-1) \frac{T}{N}\right] V_{n2}(j\omega - j\omega_0\beta)$$

where $p_n(t)$ is as in Eq. (7) and $q_n(t)$ is similar.

If $H_{xy}(j\omega)$ is selected so that

$$H_{xy}(j\omega) = 0 \quad \text{for all } |\omega| \geq \frac{\omega_0}{2}$$

then the expressions for V_{n1} and V_{n2} reduce to zero for all α and β except $\alpha = \beta = 0$; $|\omega_0\alpha| \leq \omega_0/2$ and $|\omega_0\beta| \leq \omega_0/2$ hold only when $\alpha = \beta = 0$. Thus

$$I_{n1} = \frac{1}{R_1} \sum_{\alpha} P_{\alpha} \exp\left[-j\omega_0 \alpha (n-1) \frac{T}{N}\right] \times E_1(j\omega - j\omega_0 \alpha) - \frac{1}{R_1} P_0 V_{n1}(j\omega) \quad (59)$$

$$I_{n2} = -\frac{1}{R_2} Q_0 V_{n2}(j\omega)$$

Next, by substituting the two Eqs. (59) into the Eqs. (56) and transposing the voltage terms to the left side, we obtain

$$V_{n1} \left(1 + \frac{H_{11}}{R_1} P_0\right) + V_{n2} \left(\frac{H_{12}}{R_2} Q_0\right) = \frac{H_{11}}{R_1} \sum_{\alpha} P_{\alpha} \exp\left[-j\omega_0 (n-1) \frac{T}{N}\right] E_1(j\omega - j\omega_0 \alpha) \quad (60)$$

$$V_{n1} \left(\frac{H_{21}}{R_1} P_0\right) + V_{n2} \left(1 + \frac{H_{22}}{R_2} Q_0\right) = \frac{H_{21}}{R_1} \sum_{\alpha} P_{\alpha} \exp\left[-j\omega_0 (n-1) \frac{T}{N}\right] E_1(j\omega - j\omega_0 \alpha)$$

By eliminating V_{n1} from the above equations by solving them simultaneously for V_{n2} ,

$$V_{n2}(j\omega) = \frac{1}{P_0} \Gamma(j\omega) \sum_{\alpha} P_{\alpha} \exp\left[-j\omega_0 (n-1) \frac{T}{N}\right] E_1(j\omega - j\omega_0 \alpha) \quad (61)$$

where

$$\Gamma(j\omega) = \frac{H_{21} \frac{R_2}{Q_0}}{\left(H_{11} + \frac{R_1}{P_0}\right) \left(H_{22} + \frac{R_2}{Q_0}\right) - H_{12} H_{21}} \quad (62)$$

Now it is necessary to expand the derivation to the entire network and not simply a single path. The derivation from this point will very closely parallel that of Chapter II. From Eq. (4),

$$u_2(t) = \sum_{n=1}^N v_{n2}(t) q_n(t) \quad (63)$$

and using the Laplace transform techniques shown earlier

$$U_2(j\omega) = \sum_{n=1}^N \sum_{\beta=-\infty}^{+\infty} Q_{\beta} \exp\left[-j\omega_0(n-1)\frac{T}{N}\right] \times V_{2n}(j\omega - j\omega_0\beta) \quad (64)$$

Substituting for V_{2n} , using Eqs. (61) and (62), the result is

$$U_2(j\omega) = \sum_N \sum_{\alpha} \sum_{\beta} \frac{1}{P_0} P_{\alpha} Q_{\beta} \exp\left[-j\omega_0(\alpha + \beta)(n-1)\frac{T}{N}\right] \\ \times \Gamma(j\omega - j\omega_0\beta) E_1\left[j\omega - j\omega_0(\alpha + \beta)\right] \quad (65)$$

which is similar to Eq. (12). Continuing the same method of derivation that was used on Eq. (12), it can be seen that the summation over N equals N and if $\alpha = kN - \beta$ [see Eqs. (17) and (18)], the following is obtained:

$$U_2(j\omega) = \frac{N}{P_0} \sum_{\beta} Q_{\beta} \Gamma(j\omega - j\omega_0\beta) \sum_k P_{kN-\beta} E_1(j\omega - j\omega_0kN) \quad (66)$$

and finally, by the application of the band limitations which provided Eq. (20), namely

$$E_1(j\omega) = 0 \quad \text{for all } |\omega| \geq N \frac{\omega_0}{2}$$

and

$$U_2(j\omega) = 0 \quad \text{for all } \beta \neq \pm 1$$

therefore

$$G(j\omega) = \frac{U_2(j\omega)}{E_1(j\omega)} = \frac{N}{P_0} \left[Q_{+1} P_{-1} \Gamma(j\omega - j\omega_0) + Q_{-1} P_{+1} \Gamma(j\omega + j\omega_0) \right] \quad (67)$$

It can be seen, then, that (67) is similar to Eq. (21). As was mentioned earlier, the use of the series switches in each path instead of the modulators, modulated by a unit amplitude rectangular wave has the same effect. Thus, by using Eqs. (27) and (28) to calculate P_0 , $P_{\pm 1}$, $Q_{\pm 1}$, Eq. (67) becomes

$$G(j\omega) = \frac{U_2(j\omega)}{E_1(j\omega)} = \left(\frac{\sin \frac{\pi}{N}}{\frac{\pi}{N}} \right)^2 \left[\Gamma(j\omega - j\omega_0) + \Gamma(j\omega + j\omega_0) \right] \quad (68)$$

Until now the $H(j\omega)$ function has been restricted simply to the reactive portion of a low pass filter. Now consider $H(j\omega)$ to be a single shunt capacitor as shown in Fig. 10.

$$H_{11} = \frac{1}{j\omega C} \quad H_{12} = \frac{1}{j\omega C} \quad H_{21} = \frac{1}{j\omega C} \quad H_{22} = \frac{1}{j\omega C} \quad (69)$$

and with $P_0 = Q_0 = 1/N$ from Eqs. (27) and (28)

$$\Gamma(j\omega) = \frac{\frac{1}{j\omega C} NR_2}{\left(\frac{1}{j\omega C} + NR_1 \right) \left(-\frac{1}{j\omega C} + NR_2 \right) - \frac{1}{\omega^2 C^2}} \quad (70)$$

When $R_2 \gg |1/j\omega C|$

$$\Gamma(j\omega) \approx \frac{1}{1 + j\omega NR_1 C} \quad (71)$$

and thus

$$\Gamma(j\omega \pm j\omega_0) \approx \frac{1}{1 + (j\omega \pm j\omega_0) NR_1 C} \quad (72)$$

The 3 db bandwidth can be found from Eq. (72) by

$$(\omega - \omega_0) NR_1 C = 1 \quad (73)$$

$$BW_3 \text{ db} = 2(\omega - \omega_0) = \frac{2}{NR_1 C}$$

and the Q of this filter is

$$Q = \frac{\omega_0}{BW} = \frac{\omega_0 NR_1 C}{2} \quad (74)$$

and if sensitivity is defined as

$$S_K^Q = \frac{\partial Q / \partial K}{Q/K}$$

then

$$S_{R_1}^Q = 1 \quad \text{and} \quad S_C^Q = 1 \quad (75)$$

Thus the bandwidth and the network Q are directly proportional to the number of paths in the N -path filter. Also it has been shown that the sensitivity of Q with respect to R_1 and C are both very stable, theoretically. These sensitivities are also very comparable with those of the RLC band-pass filter.

Next examine the insertion attenuation factor of Eq. (68),

$$\eta_N = \left(\frac{\sin \frac{\pi}{N}}{\frac{\pi}{N}} \right)^2 \quad (76)$$

In Fig. 12, η_N is plotted and it can be seen from the figure or Eq. (76) that for $N > 15$, $\eta_N \approx 1$.

Next, reexamine η_N after making two modifications. First, from Chapter II.B, let $N = T/\tau$, where T is the sampling period and τ

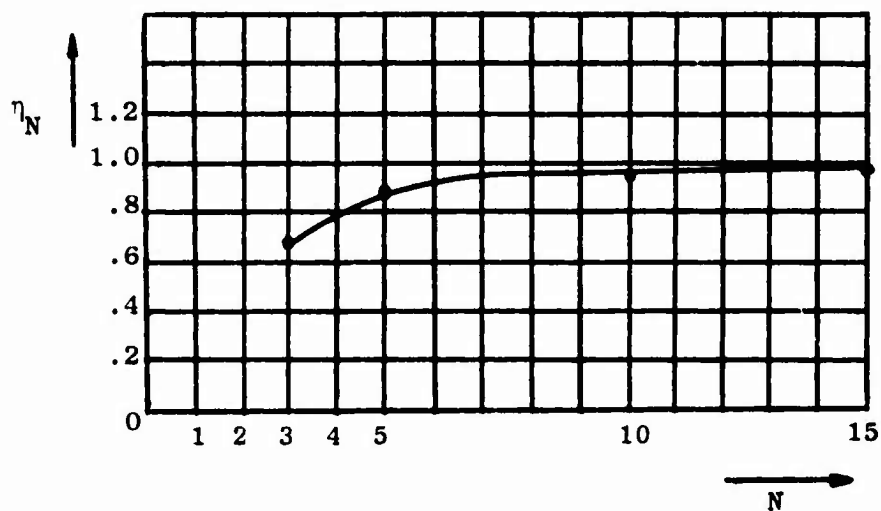


Fig. 12. INSERTION ATTENUATION η_N VERSUS N FOR A SERIES SWITCHED N -PATH FILTER.

is the sampling interval. Secondly, introduce k , an integer index to represent the harmonic number of the switching frequency. Inserting these into η_N

$$\eta_N = \left(\frac{\sin \frac{k\pi\tau}{T}}{\frac{k\pi\tau}{T}} \right)^2 \quad (77)$$

To illustrate the effect of this term, η_3 or

$$\eta_3 = \left(\frac{\sin \frac{k\pi}{3}}{\frac{k\pi}{3}} \right)^2 \quad \text{where } N = 3, \quad \frac{\tau}{T} = \frac{1}{3} \quad (78)$$

will be plotted in Fig. 13. The output spectrum of the three path filter is as shown in Fig. 14.

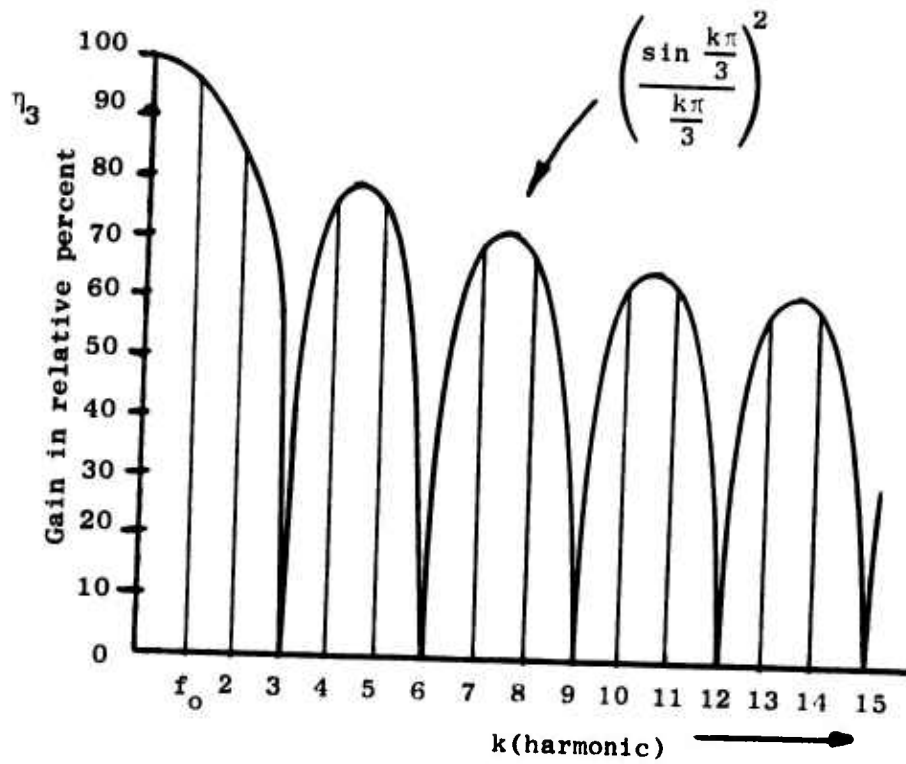


Fig. 13. HARMONIC RESPONSE ATTENUATION WITH RESPECT TO THE FUNDAMENTAL FREQUENCY FOR A THREE SECTION FILTER.

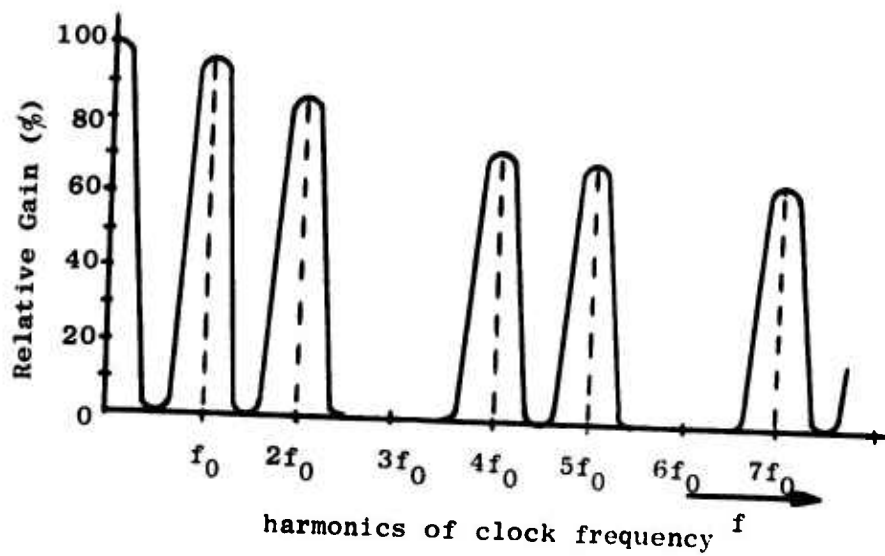


Fig. 14. FREQUENCY SPECTRUM OF A THREE PATH SWITCHED FILTER.

Thus, from the previous discussion, it can be concluded that the transfer function $G(j\omega)$ in Eq. (68), for large N will appear as a sequence of narrow, equally spaced passbands of identical shape and nearly equal height, centered at harmonics of the switching frequency ω_0 . This corresponds to the "comb filter" characteristic, which is frequently employed in the detection of periodic signals immersed in wide band noise. With an N -path filter configuration, this "comb" characteristic can easily be tuned by simply varying the switching frequency.

As a final topic before considering a shunt switching technique, the phase shift and the group time delay of this type of N -path filter will be discussed. By examining Eq. (68), it is obvious that the frequency response of the transfer function is dependent on the $\Gamma(j\omega)$ function. Thus to perform the phase angle calculation consider Eq. (72).

The phase angle is then

$$\phi(\omega) = \arctan \left[NR_1 C (\omega - \omega_0) \right] \quad (79)$$

and from $\phi(\omega)$, the group time delay is

$$\tau_G = \frac{d\phi(\omega)}{d\omega} = \frac{NR_1 C}{1 + \left[NR_1 C (\omega - \omega_0) \right]^2} \quad (80)$$

The group time delay for the 3 db bandwidth is found by using $(\omega - \omega_0) = 1/NR_1 C$ from (73) and substituting this into (80), thus

$$\tau_{G \text{ 3 db}} = \frac{NR_1 C}{1 + \left[NR_1 C \cdot \frac{1}{NR_1 C} \right]^2} = \frac{NR_1 C}{2} = \frac{1}{BW_{3 \text{ db}}} \quad (81)$$

For a simple RLC resonate circuit, these same functions are as follows:

Thus shunt switching will reduce the number of switches by a factor of two. Also by using a single shunt switch in place of the two series switches, the problems that arise from nonidentical switches in the same filter leg will be eliminated (this problem will be discussed further in Chapter VI).

As will be seen in Chapter VI, by the use of active filter techniques, it is possible to overcome the tolerance problems to be discussed in Chapter V. These active circuit configurations lend themselves almost exclusively to the shunt switching configuration, thus further discussion of this point will be deferred until then.

BLANK PAGE

Chapter V

N-PATH REALIZATION PROBLEM

In this section the effects of trying to realize an N-path filter with non-ideal components subject to production tolerances will be determined. It will be shown that these tolerances cause two interfering signals to appear at the filter output; namely a portion of the switching frequency f_0 and the frequency difference $2f_0 - f_{\text{desired}}$. It will also be shown that the signal to noise ratio customarily demanded, would lead to non-realizable close production tolerances. This ratio depends on the mutual agreement of the N paths with respect to the amplitude and phase of their transfer function, and on the quality of the switching pulses. The major portion of this discussion was developed by E. Langer [LA2] and in his development, he has presented several approaches that minimize the tolerance difficulties to some degree. Also, in this section, some consideration of the selectivity problems presented by the use of simple RC networks is discussed.

A. Interference Effect

From the mathematical treatment of the network in Chapter II, assuming that $H(j\omega)$ represents the transfer function of a low pass filter, and the switches and switching impulses are identical, the output function can be represented as in Eq. (4) or

$$u_2(t) = \sum_{n=1}^N q_n(t)v_n(t) = \sum_{n=1}^N q_n(t) \left[h(t) * (p_n(t) \cdot u_1(t)) \right] \quad (83)$$

In Eq. (83) all $h(t)$'s are assumed identical, and $p_n(t)$ and $q_n(t)$ are the switching functions of M_1 and M_2 , the input and output modulators. See Fig. 16 for a pictorial representation of the terms for a single path. The next step is to generalize the above result to the situation where the filters are non-ideal due to component tolerances. The expression in Eq. (83) generalizes to

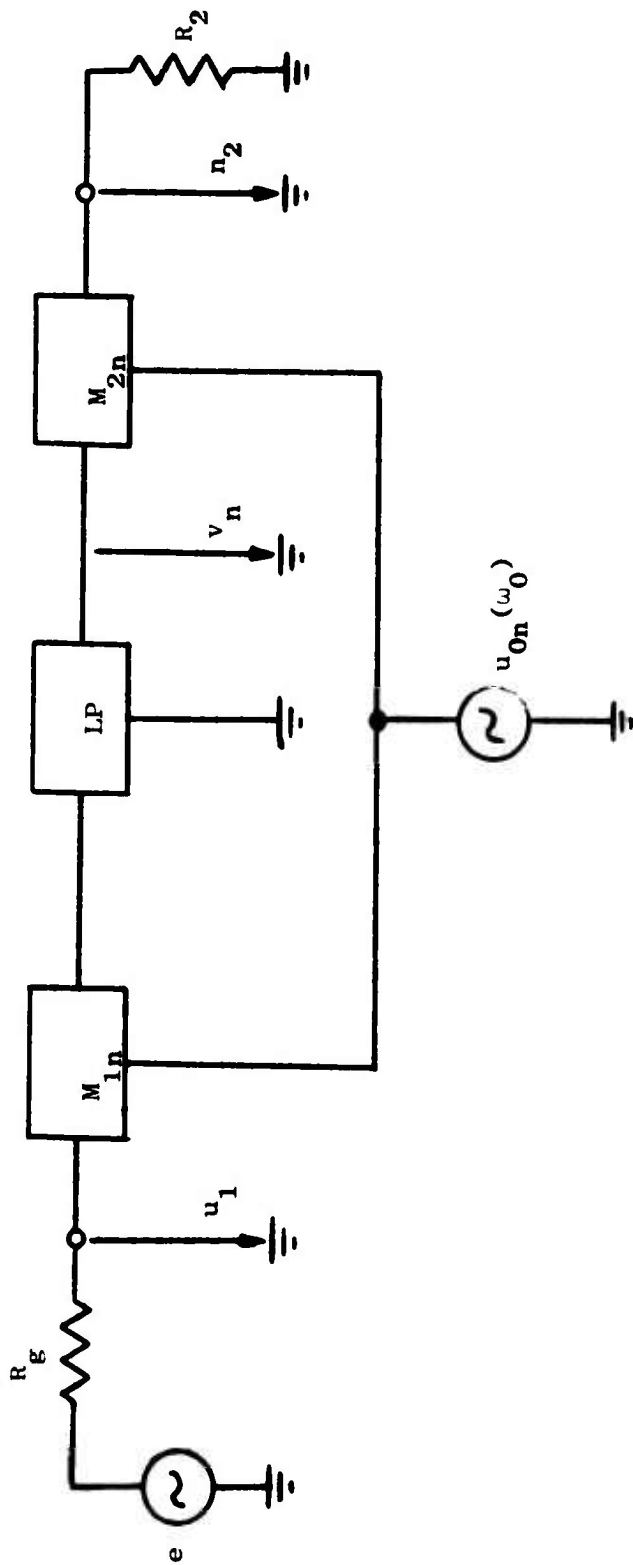


Fig. 16. GENERALIZATION OF A SINGLE PATH OF AN N-PATH FILTER SHOWING THE VOLTAGE NOTATION AND INCLUDING INPUT AND OUTPUT SERIES MULTIPLIERS.

$$\begin{aligned}
u_2(t) = & q_1(t) \left[h_1(t) * (p_1(t) \cdot u_1(t)) \right] \\
& + q_2(t) \left[h_2(t) * (p_2(t) \cdot u_1(t)) \right] \\
& + q_3(t) \left[h_3(t) * (p_3(t) \cdot u_1(t)) \right] + \dots
\end{aligned} \tag{84}$$

Before making the calculations necessary to determine the extent of the interference due to the switching functions and the network components, it would be wise to make several qualitative considerations beforehand. As was developed in Chapter IV, the transfer function of the N-path filter is dependent on all of the harmonics of the modulating frequency ω_0 . Since the notation required by the following discussion is somewhat different from previous notation, a brief derivation of the harmonic content will be introduced at this time.

The Fourier analysis of a rectangular impulse of amplitude 1, width τ and the repetitive frequency

$$f_0 = \frac{1}{T} = \frac{1}{N\tau} \quad \text{with} \quad \tau = \frac{T}{N} \tag{85}$$

leads to the spectrum

$$\begin{aligned}
U(\omega_0) &= \frac{2 \sin \frac{\pi}{N}}{\pi} \triangleq U_{0,n} \\
U(2\omega_0) &= \frac{2 \sin \frac{2\pi}{N}}{2\pi} \\
U(3\omega_0) &= \frac{2 \sin \frac{3\pi}{N}}{3\pi} \\
U(\nu\omega_0) &= \frac{2 \sin \frac{\nu\pi}{N}}{\nu\pi}
\end{aligned} \tag{86}$$

Each of these harmonics of ω_0 leads to a low-pass to band-pass transformation. Thus the performance of the network may be investigated for each harmonic of the modulating frequency separately.

The temporal displacement of modulating frequency from path to path has the phase angle

$$\varphi_n = (n - 1) \frac{2\pi}{N} \quad (87)$$

The signal behavior of a single path n , with the oscillator voltage

$$u_{0,n}(t) = U_{0,n} \cos(\omega_0 t + \varphi_n) = \frac{1}{2} U_{0,n} \cdot \sum_{\nu=\pm 1} \exp[j\nu(\omega_0 t + \varphi_n)] \quad (88)$$

and the input voltage

$$u_1(t) = U_1 \cos \omega_1 t = \frac{1}{2} U_1 \cdot \sum_{\nu=\pm 1} \exp[j\nu\omega_1 t] \quad (89)$$

can be described as follows:

$$u_{2,n}(t) = \left\{ \frac{1}{4} \left[U_{0,n} \sum_{\nu=\pm 1} \exp[j\nu(\omega_0 t + \varphi_n)] \right] U_1 \sum_{\nu=\pm 1} \exp(j\nu\omega_1 t) \right\} * h(t) \quad (90)$$

$$\cdot \frac{1}{2} U_{0,n} \sum_{\nu=\pm 1} \exp[j\nu(\omega_0 t + \varphi_n)]$$

In the real filter it is possible that the two multipliers would be different, however, the worst case effect of the tolerances occurs when both multipliers are equal. The first multiplication in Eq. (90) (in square brackets) conveys that

$$u_1(t) \cdot u_{0,n}(t) = \frac{1}{4} U_{0,n} \cdot U_1 \left\{ \sum_{v=\pm 1} \exp \left[jv(\omega_0 t + \varphi_n + \omega_1 t) \right] \right. \\ \left. + \sum_{v=\pm 1} \exp \left[jv(\omega_0 t + \varphi_n - \omega_1 t) \right] \right\} \quad (91)$$

In the present case, only a single filter input frequency produces this interesting condition. Permitting the convolution of the expression in Eq. (91) with $h_n(t)$, produces the transformation of $H_n(j\omega_1)$ to $H_n(j(\omega_0 \pm \omega_1))$. By definition, the transfer function of the low pass element is

$$H_n(j\omega) = H_n(\omega) \exp \left[j\varphi_n(\omega) \right] \quad (92)$$

with

$$H_n(\omega) = |H_n(j\omega)|$$

and

$$\varphi_n = \arctan \frac{\text{Im } H_n(j\omega)}{\text{Re } H_n(j\omega)}$$

and if $\omega = \omega_0 \pm \omega_1$

$$H_n \left[j(\omega_0 \pm \omega_1) \right] = H_n(j\omega)_{\omega=\omega_0 \pm \omega_1}$$

If the low pass upper frequency limit ω_g is much smaller than ω_0 , then for all practical purposes the $\omega_0 + \omega_1$ terms in the output voltage are negligibly small. The voltage $v_n(t)$ which is a function of the magnitude and phase of $H_n(j\omega)$ can be represented as

$$v_n(t) \approx k_n \sum_{v=\pm 1} \exp \left[jv(\omega_0 - \omega_1)t + \varphi_n + \varphi_n \right] \quad (93)$$

in which case

$$k_n = H_n(\omega_0 - \omega_1) = \left| H_n(j\omega)_{\omega=\omega_0-\omega_1} \right|$$

and

$$\delta_n = \arctan \frac{\text{Im } H_n(j\omega)_{\omega=\omega_0-\omega_1}}{\text{Re } H_n(j\omega)_{\omega=\omega_0-\omega_1}}$$

for this selection, the transfer gain and the phase angle of a single path are determined. From this expression of $v_n(t)$, the path output voltage of the form is obtained:

$$\begin{aligned} u_{2,n}(t) &\approx \frac{1}{8} U_{0,n}^2 U_{1,n} k_n \left\{ \sum_{v=\pm 1} \exp \left[jv \left((2\omega_0 - \omega_1)t + 2\phi_n + \delta_n \right) \right] \right. \\ &\quad \left. + \sum_{v=\pm 1} \exp \left[jv \left(-\omega_1 t + \delta_n \right) \right] \right\} \quad (94) \\ &= \frac{1}{4} U_{0,n}^2 U_{1,n} k_n \left\{ \cos \left[(2\omega_0 - \omega_1)t + 2\phi_n + \delta_n \right] + \cos \left[\omega_1 t - \delta_n \right] \right\} \end{aligned}$$

It is now evident that the output voltage of a single path $u_{2,n}$ contains two components, one with the signal frequency ω_1 and the other is a function of $2\omega_0 - \omega_1$. When the effect of the series switch is considered on the single path reaction, there is the effect of the constant voltage component A_n of the switch introduced while conducting into the $u_{2,n}$ term. This new component is a function of the form $U_{0,n} A_n \cos(\omega_0 t + \phi_n)$.

Thus, in order to get the output voltage for the entire N-path filter, it is necessary to simply sum all of the $u_{2,n}$ functions together and get:

$$\begin{aligned}
u_2 &= \sum_{n=1}^N u_{2,n}(t) \\
&\approx \frac{1}{4} U_{0,1}^2 U_1 k_1 \left\{ \cos \left[(2\omega_0 - \omega_1)t + 2\varphi_1 + \varepsilon_1 \right] + \cos \left[\omega_1 t - \varepsilon_1 \right] \right\} \\
&\quad + U_{0,1} A_1 \cos (\omega_0 t + \varphi_1) + \frac{1}{4} U_{0,2}^2 U_1 k_2 \left\{ \cos \left[(2\omega_0 - \omega_1)t + 2\varphi_2 + \varepsilon_2 \right] \right. \\
&\quad \left. + \cos \left[\omega_1 t - \varepsilon_2 \right] \right\} + U_{0,2} A_2 \cos (\omega_0 t + \varphi_2) + \dots
\end{aligned} \tag{95}$$

In the ideal filter $U_{0,1} = U_{0,2} = \dots = U_{0,N}$, $k_1 = k_2 = \dots = k_N$, $\varepsilon_1 = \varepsilon_2 = \dots = \varepsilon_N$ and $A_1 = A_2 = \dots = A_N$, moreover, Eq. (87) is exactly valid and the $2\omega_0 - \omega_1$ and the ω_0 terms disappear from $u_2(t)$, such that

$$\begin{aligned}
u_2(t) &\approx \frac{1}{4} U_0^2 U_1 k \cos (\omega_1 t - \varepsilon) + \frac{1}{4} U_0^2 + U_1 k \cos (\omega_1 t - \varepsilon) + \dots \\
&= \frac{1}{4} U_0^2 U_1 k N \cos (\omega_1 t - \varepsilon)
\end{aligned} \tag{96}$$

Thus, by examination of Eq. (95), it is seen that the size of the disturbance voltage in a real filter is dependent of five parameters.

1. The difference in the oscillation amplitude $U_{0,n}$ caused by unequal pulse widths of the keying impulse;
2. The difference in the damping factor k_n of the paths;
3. The difference in the phasing ε_n of the paths, which is caused chiefly by the tolerance of the RC low pass components;
4. The deviation of the keying impulse phasing φ_n depending essentially on the accuracy of the key impulse generator.
5. The inequality of the quiescent points, the betas, the saturation voltages, and the switching and storage times of the transistor switches.

B. Discussion of Means to Minimize the Interference Effect

From the above list, it is clear that the disturbance in an N-path filter is primarily one of the interactions of one path with another, and not just the result of the tolerance of a single path. From these circumstances it is also very clear that certain of these filter elements are particularly suited to integration. By integration, several nearly equivalent transistors or RC-networks can be produced on a single substrate and then be used as building blocks. Thus temperature variations will have an equivalent effect on all paths, so that it might be expected that the filter quality would remain constant over a usable range of temperatures. Just as important as the temperature swing, is the variation in the long time constant of particular filter components. By merely integrating the circuits onto a single substrate does not hold the component value tolerances to within a useable range, thus it is necessary to use a more complicated combination of integration techniques.

By a critical examination of the five methods of error injection listed in the last section, it is clear that the component tolerances have a sufficiently small effect on errors discussed in points 1 and 4. The higher the operating frequency of the filter, the greater the need for matched transistor switches and on the overall quality of the keying impulses. For these reasons, the realization of the N-Path Filter has an upper operating frequency limit of about 2 MHz at the present time.

If parallel switching is introduced in place of the series switches, for which the above equations were developed, then the cause of the keying impulse errors is chiefly the collector-base capacitance of the switching transistor. The effect of using parallel switching is to weaken the factors A_n in Eq. (95). Let this weakened factor be a_n .

An effective method, introduced by Langer [LA2], for the reduction of the keying impulse disturbance is achieved by using a push-pull/single-ended configuration as shown in Fig. 17. In this configuration, the switching impulse switches both sides of the N-path channels at the same time, by so doing, this leads to compensation of the keying impulse largely through the differential output of the filter.

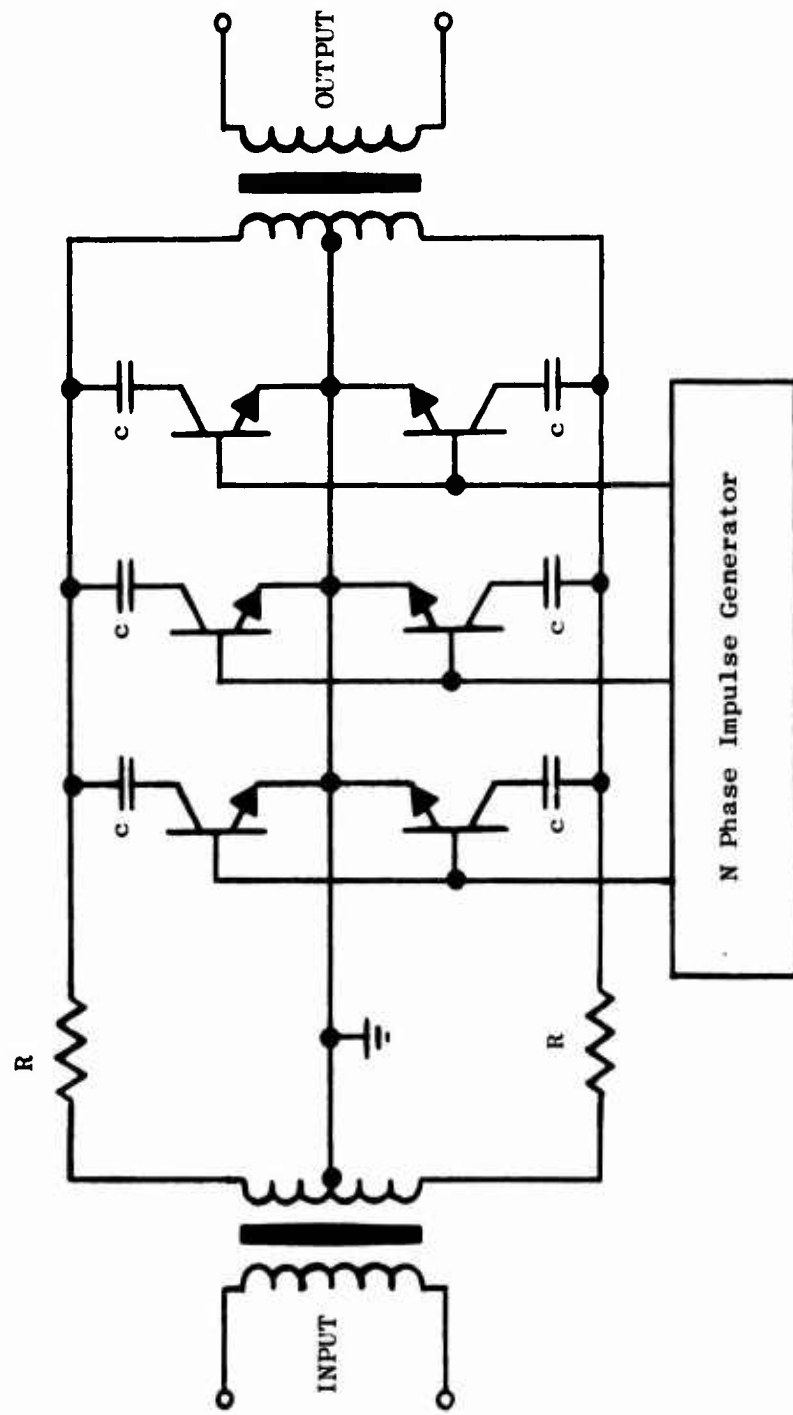


Fig. 17. THREE-PATH SINGLE-ENDED/PUSH-PULL CONFIGURATION.

The simplest method for the removal of the characteristic disturbance of N-path filters is the synchronization of the switching pulse generator with the wanted signals. Then the switching frequency and the reflected frequency are equal to the wanted signal frequency. In this situation, the disturbances reduce to a small modulation gradient.

C. The Selectivity Problem

The N-path filter for the low-pass-bandpass transformation is dependent on the selection of low-pass filter sections, $H(s)$, for their quality, Q . If the low-pass element is a simple RC, then the skirts drop off at the rate of 6 dB per octave at best, which is not sufficient. The transfer function of a simple well behaved low-pass section has only one real pole. By cascading several RC sections the skirts become steeper at the rate of approximately 6 dB per octave for each additional section (the 6 dB factors are of course additive). Likewise, as the component count increases, the bandwidth of the low-pass filter very rapidly approaches its limit. As is well known, by cascading simple RC sections, it is impossible to achieve anything other than poles on the real axis for the low-pass filters.

In order to attain a favorable relationship between bandwidth and selectivity, at least one pair of complex conjugate poles is necessary. Thus the denominator polynomial of the transfer function must be of at least order 2, and its roots must consist of complex conjugate roots in pairs. As is also well known, the transfer function of a network must be a rational function and be of the form

$$G(s) = \frac{a_0 + a_1 s + a_2 s^2 + \dots + a_n s^n}{b_0 + b_1 s + b_2 s^2 + \dots + b_m s^m} = \frac{Z(s)}{P(s)} \quad (97)$$

$$s = \sigma + j\omega$$

Assuming $G(s)$ is as simple as possible, $P(s)$ must be of order two and its roots must also consist of a complex conjugate pole pair, thus

$$\left(\frac{b_1}{b_2}\right)^2 = 4 \frac{b_0}{b_2} \quad (98)$$

In some cases it may also be desirable to have complex conjugate zero pairs. In the case where there are both complex zeros and poles, the network can be realized by using the passive bridge tee configuration. As was seen earlier, the low-pass-bandpass transformation retains the symmetry of the pole pairs and transforms them to around $\pm j\omega_0$ instead of 0.

An active low-pass filter of order three can be easily realized as shown in several configurations by Sallen and Key [SA1]. More will be said about this in the next chapter on applications.

When active low-pass filters are used in the paths, it is necessary to reexamine some of the characteristics of the transfer function. There is particular interest in determining the damping function. For this calculation, assume a path configuration as shown in Fig. 18 with the frequency approaching zero. From Eqs. (58) and (62) it can be considered that the transfer function $G(j\omega)$ approaches the product of two factors; $[\sin(\pi/N)/(\pi/N)]^2$ and $\Gamma(j\omega)$. With $P_0 = Q_0 = 1/N$, then

$$\Gamma(j\omega) = \frac{H_{21} R_2 N}{(H_{11} + R_1 N)(H_{22} + R_2 N) - H_{12} H_{21}} \quad (99)$$

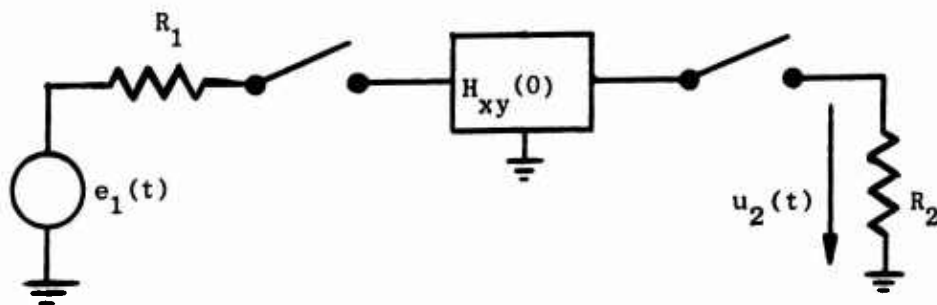


Fig. 18. SINGLE PATH CONFIGURATION.

Then for $\omega = 0$ and $R_2 = \infty$

$$P(0) = \frac{H_{21}(0)}{H_{11}(0) + R_1 N} \quad (100)$$

Thus the damping argument of the filter is

$$\gamma_N = \frac{U_2(\omega)_{\omega 0}}{E_1(\omega)_{\omega 0}} = \frac{\sin^2 \frac{\pi}{N}}{\left(\frac{\pi}{N}\right)^2} \cdot \frac{H_{21}(0)}{H_{11}(0) + R_1 N} \quad (101)$$

It can be seen that the feedback in an active filter will add some regulation and reduce the effect of component tolerances on the stability of the circuit. The tolerance sensitivity of such a network increases quickly for $n > 3$, likewise the size of the substrate used to integrate the filters and switches grows so large that homogeneity is less likely and the yield becomes poorer.

Because of the periodicity of the frequency spectrum of the N-path-filter, as shown in Fig. 14, it becomes essential that the quality of the wideband filter which follows the N-path-filter is dependent on the far-off selectivity of the low-pass filters. With respect to the cross modulation disturbances, a selection should be made such that a portion of the theoretically desired selectivity is achieved from these disturbances. The requirements for the skirt roll-off of the theoretical series wide-band filter depends directly on, among other things, the number of paths, N. This dependence can be seen by examining the plots of the damping function γ_N in Fig. 19. For small N, γ_N drops off rapidly as the harmonic number increases, and for larger N the damping reduces much slower as the harmonic number increases. The formula for the required theoretical selectivity S_z is

$$S_z \geq S - 20 \log \frac{r^2 \sin^2 \frac{\pi}{N}}{\sin^2 r \frac{\pi}{N}} \text{ dB} \quad (102)$$

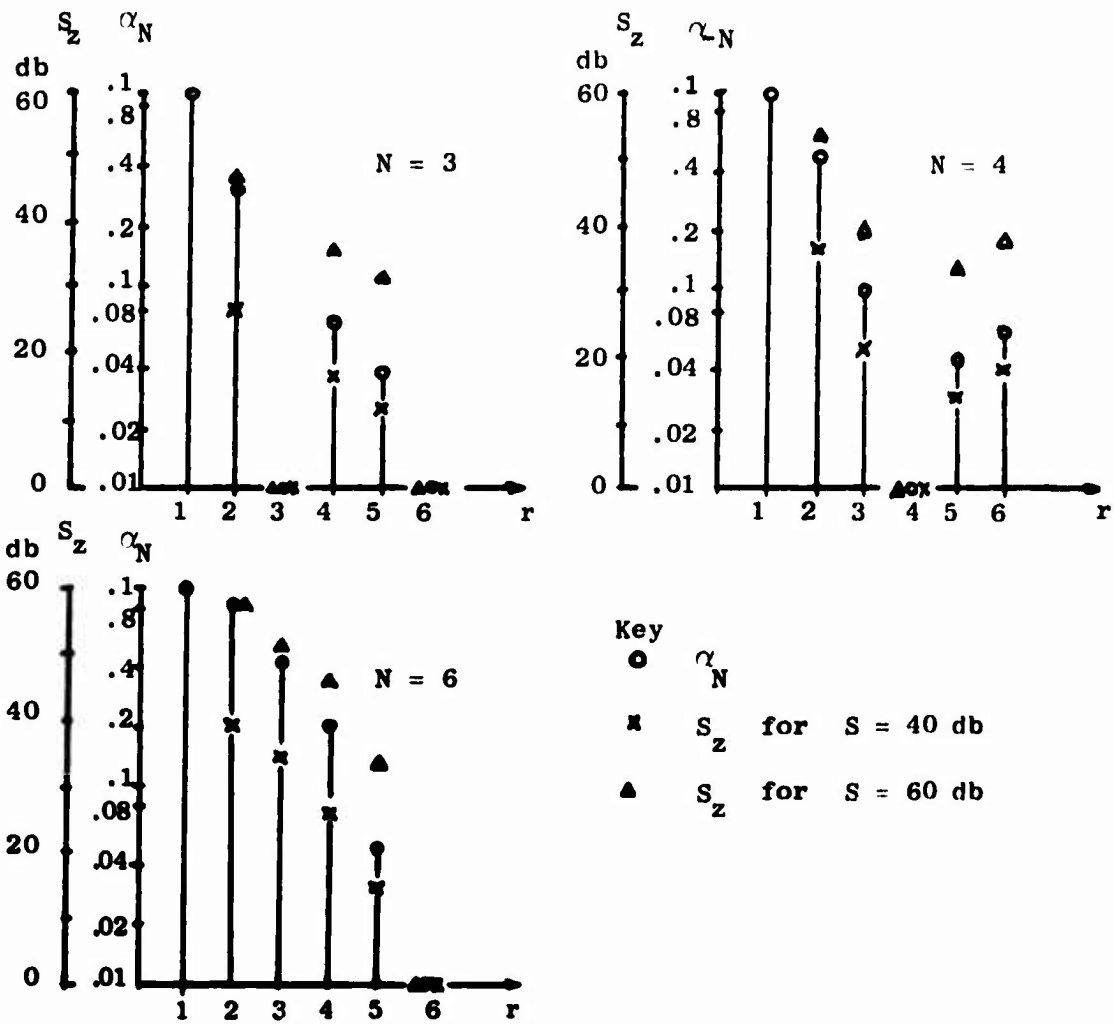


Fig. 19. RELATIVE DAMPING AND SELECTIVITY FOR A N-PATH FILTER.

where

S = desired far-off selectivity

r = harmonic number of ω_0

This also is plotted in Fig. 19. Thus, the far-off selectivity becomes poorer as N increases and the following wideband filter and the low pass filters in the individual paths must be sharper and thus become more difficult to realize.

BLANK PAGE

Chapter VI

APPLICATIONS

In this chapter the performance characteristics of N-path filters and why it would be advantageous to use this configuration over some other will be discussed. Also, several specific examples of practical applications for the N-path filter will be given.

From past experience it is well known that high Q bandpass filters at relatively low frequencies require large inductors, and as a general rule, are impractical since Q is limited to approximately 100 by these inductors. The filters also tend to be very sensitive to small changes in element values. As was shown in the development of the performance factors of the N-path-filter in the earlier sections, the N-path filter can overcome many of these objections.

The performance characteristics of the N-path filter that make their potential use attractive in general and for some specialized applications are:

- 1) Periodic filtering characteristics can be achieved over a limited frequency band, thus realizing a low-frequency comb filter response without using distributed elements.
- 2) Narrow-band band-pass and band-elimination filters can be realized at very low frequencies without the use of inductors.
- 3) A low-pass to band-pass transformation can be realized exactly.
- 4) The center frequency and the bandwidth (as will be seen in the following implementation) of the resultant filter can be varied electronically.

Although interest in this method of "commutating" a set of low pass filters into a bandpass or comb filter appeared as early as 1953, it was not feasible for most applications before solid state switches became available to replace mechanical commutators. By integrating the filters and the switches, the present state of the technology will allow:

- 1) the operation of an N-path filter from approximately 3 Hz to 2 MHz
- 2) excellent temperature stability
- 3) small size and weight.

Thus as was shown throughout this paper and in the literature, the N-path-filter has been of interest for many reasons. In summary, some of these reasons were:

- 1) The comb filter characteristic which could be achieved at low frequencies as well as a higher frequency
- 2) Possibly realizing an all-pass constant delay network over a limited bandwidth without inductors (Franks and Sandberg [FR1])
- 3) Narrow-band-band-pass filter over a considerable frequency range with a high Q and small size. Electronically variable center frequency and bandwidth may also be included.
- 4) Also, from the observations in Chapter III, by using other than low-pass filters in the N-paths it is possible to design a variable attenuator, a notch filter and a pair of adjacent band-pass filters with a notch between them by using a simple high-pass filter, a first order all-pass section and a simple band-pass filter respectively.

A. Implementation Example

The implementation example to be presented next is a very interesting and recent design which was the topic of two papers by E. Langer [LA3], [LA4]. This implementation employs an N-path filter in the I.F. of an AM/FM receiver with electronic bandwidth switching. The receiver is being produced by Siemens of West Germany. A block diagram of the integrated receiver is shown in Fig. 20.

In Chapter 5 it was shown that tolerance and stability problems require that the individual path low-pass filters have complex conjugate poles. The second order active low-pass filter that will be used as the basic functional unit for the N-path filter in this implementation is shown in Fig. 21. The transfer function is developed as follows:

$$G_1(s) = \frac{V_2(s)}{V_1(s)} = \frac{1}{1 + sR_1C_1}, \quad G_2(s) = \frac{V_4(s)}{V_3(s)} = \frac{1}{1 + sR_2C_2} \quad (103)$$

$$V_4(s) = -V_1(s) G_1(s) a_1 G_2(s) \quad (104)$$

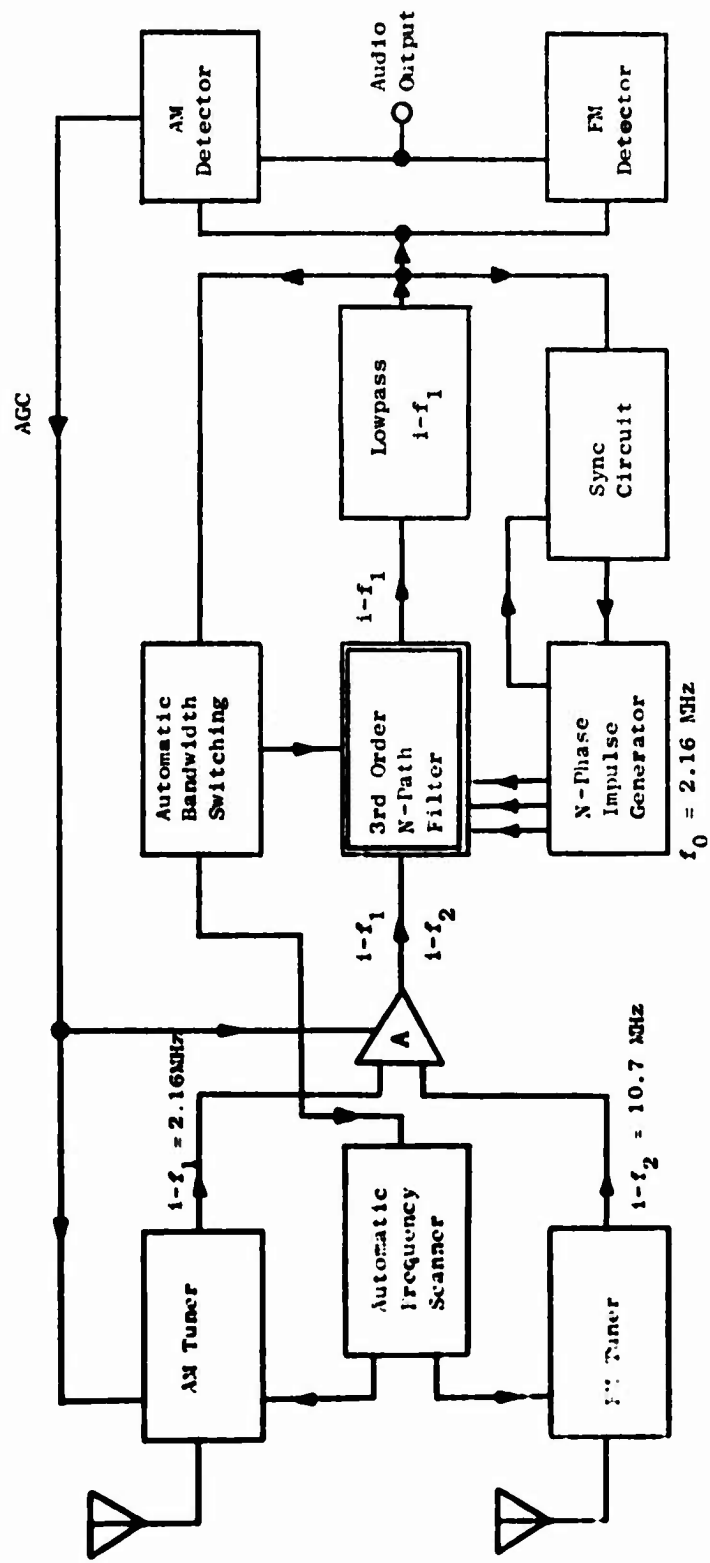


FIG. 20. AM/FM INTEGRATED RECEIVER.

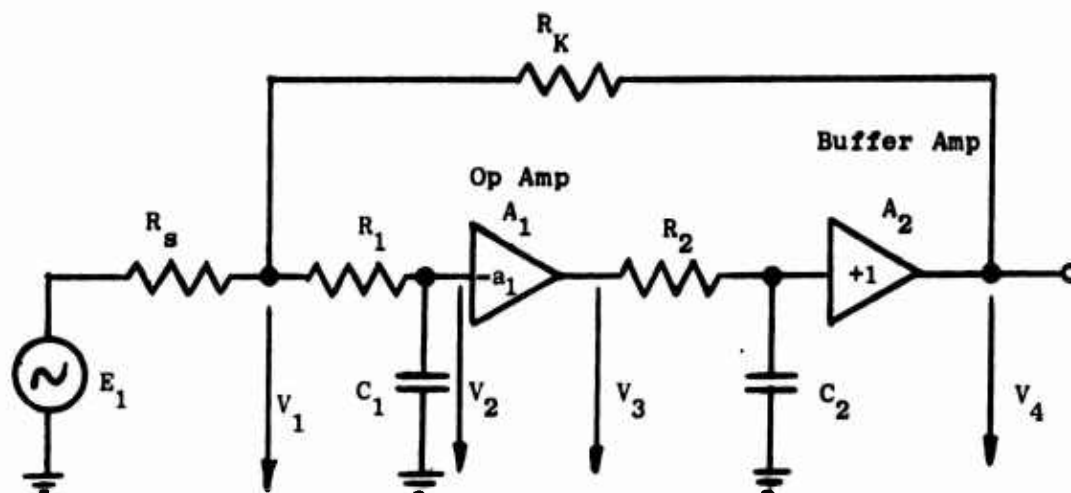


Fig. 21. ACTIVE SECOND ORDER LOW-PASS FILTER.

Assuming $R_1 \gg R_K$, $R_1 \gg R_g$

$$V_4(s) \approx - \left(E_1(s) \frac{R_K}{R_s + R_K} + V_4(s) \frac{R_s}{R_s + R_K} \right) G_1(s) a_1 G_2(s) \quad (105)$$

Thus the overall transfer function is

$$F(s) = \frac{V_4(s)}{E_1(s)} \approx \frac{-R_K}{\frac{R_s + R_K}{a_1 G_1(s) G_2(s)} + R_s} \quad (106)$$

and substituting for $G_1(s)$ and $G_2(s)$

$$F(s) \approx \frac{-1}{\frac{R_s + R_K}{R_K a_1} \left[1 + s(R_1 C_1 + R_2 C_2) + s^2 \cdot R_1 C_1 R_2 C_2 \right] + \frac{R_s}{R_K}} \quad (107)$$

For $F(s)$ to be the transfer function with two complex conjugate poles, the discriminant of the denominator must be less than zero, or

$$\frac{(R_1 C_1 + R_2 C_2)^2}{4R_1 C_1 R_2 C_2} < 1 + \frac{R_s a_1}{R_s + R_K} \quad (108)$$

By replacing the capacitors in Fig. 21 with switched triplets of capacitors, the configuration is converted to a variable-time filter with N-path character. Thus, the low-pass filters are transformed to bandpass filters in accordance with the N-path rules developed in previous sections. The net effect is that each $G(s) = 1/(1+sRC)$ is replaced by

$$G(s \pm j\omega_0) = \frac{\sin^2\left(\frac{\pi}{N}\right)}{\left(\frac{\pi}{N}\right)^2} \left[\frac{1}{1 + (s-j\omega_0)NRC} + \frac{1}{1 + (s+j\omega_0)NRC} \right] \quad (109)$$

assuming that rectangular modulation is employed. Entering two functions of this form into Eq. (106), and after some reordering, the transfer function of a second-order bandpass filter shown in Fig. 22 is obtained.

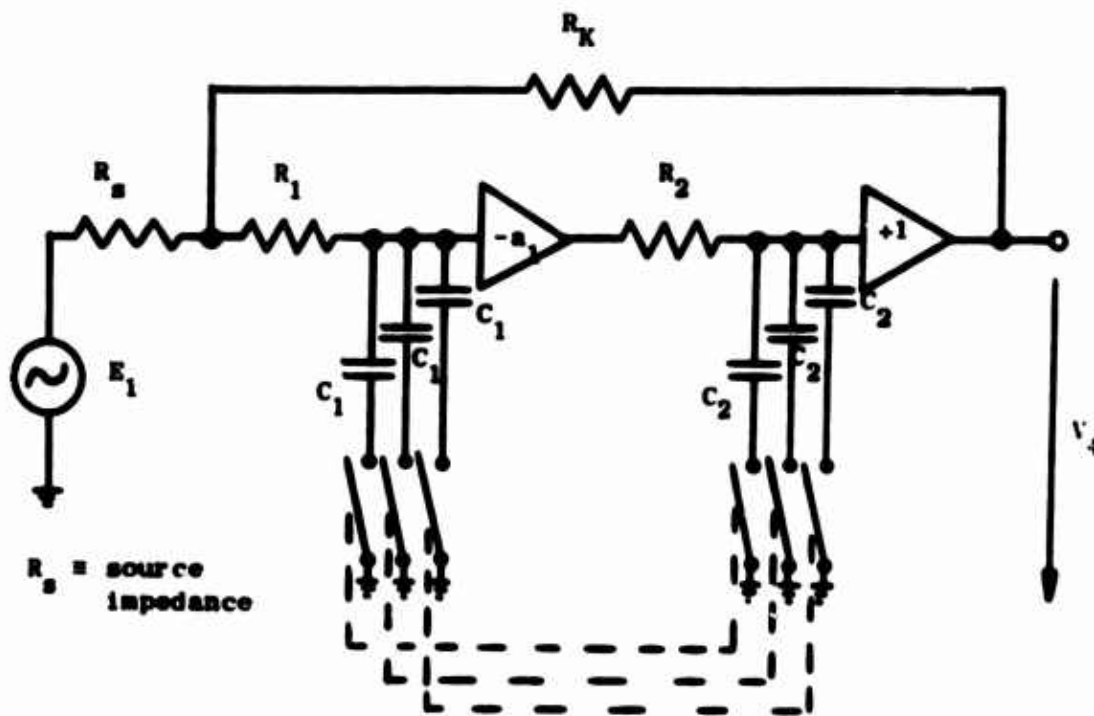


Fig. 22. ACTIVE SECOND ORDER 3-PATH FILTER.

$$\begin{aligned}
F_N(s) &= \frac{V_4(s)}{E_1(s)} \approx \frac{-R_K}{\frac{R_s + R_K}{a_1 k^2 \left[\frac{1}{1 + (s - j\omega_0)NR_1C_1} \cdot \frac{1}{1 + (s - j\omega_0)NR_2C_2} \right]} + R_s} \\
&= \frac{-1}{\frac{R_s + R_K}{a_1 R_K k^2} \left[1 + (s - j\omega_0)N(R_1C_1 + R_2C_2) + (s - j\omega_0)^2 N^2 R_1C_1R_2C_2 \right] + \frac{R_s}{R_K}}
\end{aligned} \tag{110}$$

where $k = [\sin^2(\pi/N)]/(\pi/N)^2$ and interest has been limited to the upper half of the s -plane. Location of the poles can be made by studying the denominator of Eq. (110). First let $R_s/(R_s + R_K) = \lambda$ and $s - j\omega_0 = p$. Now solve

$$p^2 N^2 R_1 C_1 R_2 C_2 + pN(R_1 C_1 + R_2 C_2) + 1 + a_1 k^2 \lambda = 0 \tag{111}$$

for p .

$$p_{1,2} = -\frac{R_1 C_1 + R_2 C_2}{2NR_1 C_1 R_2 C_2} \pm \sqrt{\frac{(R_1 C_1 + R_2 C_2)^2}{4N^2 (R_1 C_1 R_2 C_2)^2} - \frac{1 + a_1 k^2 \lambda}{N^2 R_1 C_1 R_2 C_2}} \tag{112}$$

Thus, for Fig. 23

$$\begin{aligned}
J_{\text{pole}} &= -\frac{R_1 C_1 + R_2 C_2}{2NR_1 C_1 R_2 C_2} \\
J_{-1,2} &= +j \sqrt{\frac{(R_1 C_1 + R_2 C_2)^2}{4N^2 (R_1 C_1 R_2 C_2)^2} - \frac{1 + a_1 k^2 \lambda}{N^2 R_1 C_1 R_2 C_2}} + j\omega_0
\end{aligned} \tag{113}$$

and $J_{-3,4} = J_{-1,2}^*$

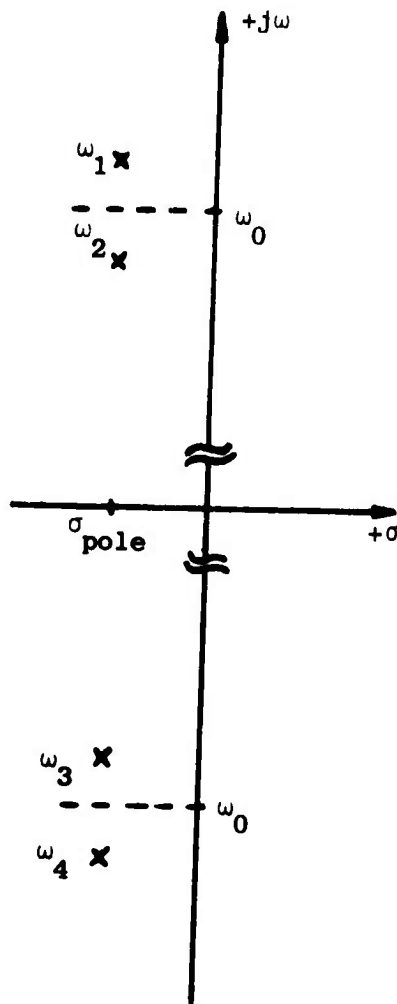


Fig. 23. s-PLANE PLOT OF N-PATH FILTER POLES.

The $\omega_{1,2,3,4}$ equations require the condition

$$\frac{(R_1 C_1 + R_2 C_2)^2}{4R_1 C_1 R_2 C_2} < 1 + a_1 k^2 \lambda \quad (114)$$

for the pole plot to be as shown in Fig. 23.

Thus, the real component of the pole locations is only dependent on the low-pass time constants and the number of paths. The imaginary component, on the other hand, is dependent on the network amplification and the source and feedback impedances as well.

The results of a qualitative analysis, performed by Langer [1A3], yields a voltage gain of 20 to 40 dB, which can be realized with relatively simple circuitry and suffices for practical requirements. It is necessary that care must be taken to minimize amplifier phase shift in the vicinity of the switching frequency, ω_0 . Also, since the network is time-variable, no delay or storage effects can be tolerated without deterioration of the rf response and the overall gain.

By cascading an additional N-path section, as shown in Fig. 24, the new filter becomes a third order bandpass filter with a nearly flat area in the middle of the response curve. With the network structured as shown in Fig. 24, the active circuits are common to all paths, thus the center frequency and the inherent filter noise are not affected by the parameter deviations of the operational amplifiers. An improvement in the signal-to-noise ratio, as well as, a sharper selectivity curve is ensured by placing the op amp between the keyed low-pass networks.

Further analysis of the circuit in Fig. 24 reveals that the bandwidth of the filter can be varied by a ratio of 1:10 by varying R_1 and R_2 . For larger ratios, the capacitors must be varied as well. Thus, electronic control of the filter bandwidth can be achieved by varying R_1 and R_2 , and a suitable circuit for this is introduced in Fig. 25.

Since in this integrated receiver the conventional ratio detector is replaced by an inductorless demodulator circuit, there is no suitable tuning criterion. By using bandwidth switching in the N-path filter, the transfer function of the filter may be adjusted first while tuning to a narrow bandwidth and then automatically switched to the specified value when the proper tuning position is achieved.

The AM tuning accuracy can similarly be improved by synchronizing the N-path filter with the desired signal. If, during tuning, the bandwidth of the receiver is made narrow enough and increased to full channel width as soon as the pulse generator is synchronized, a ratio of the locking range to the pull in range of 3 to 5 is achieved. This 3 to 5 compares quite favorably to the pull-in range factor of 2 for "flywheel synchronization" circuits (see Fig. 26).

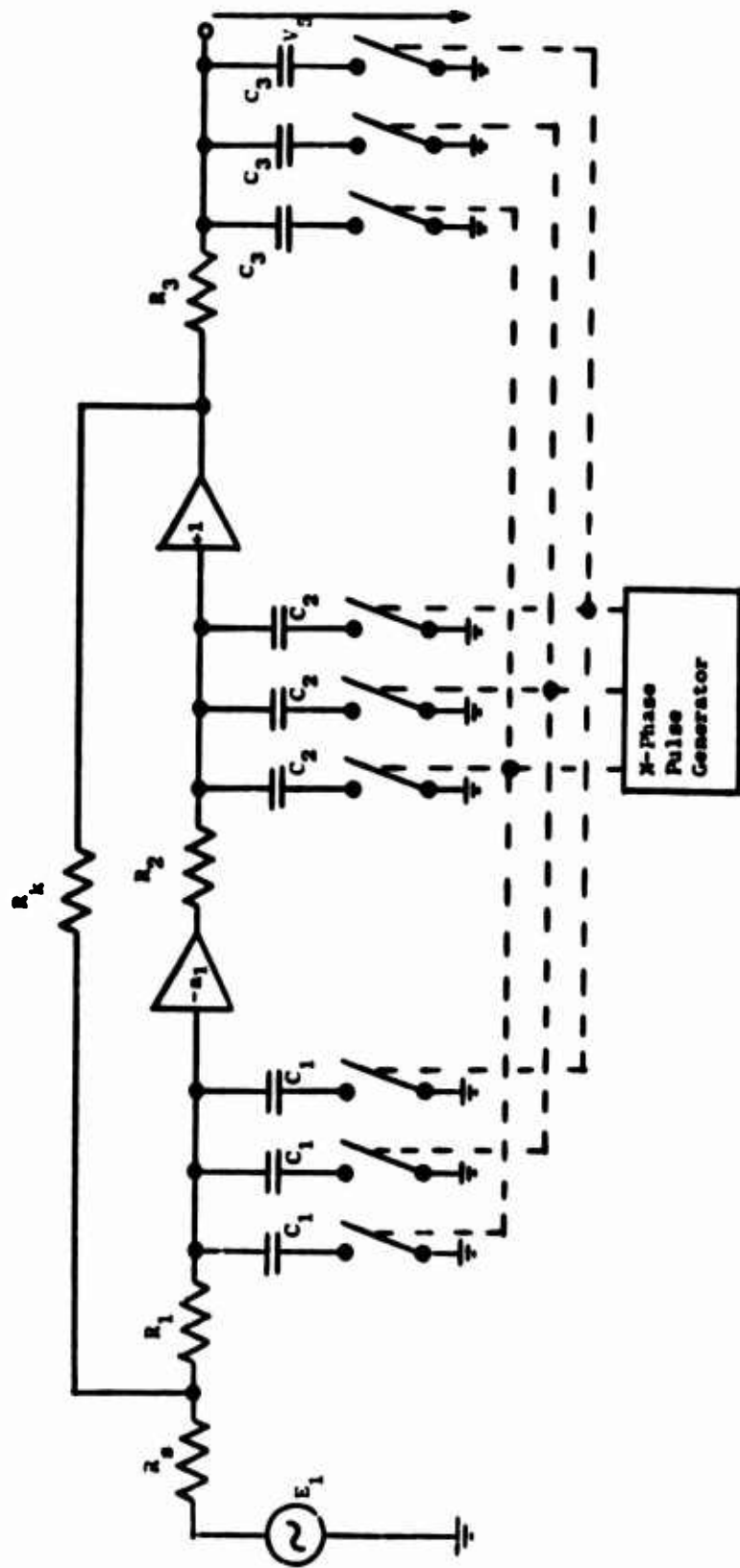


FIG. 24. THIRD ORDER 3-PATH FILTER.

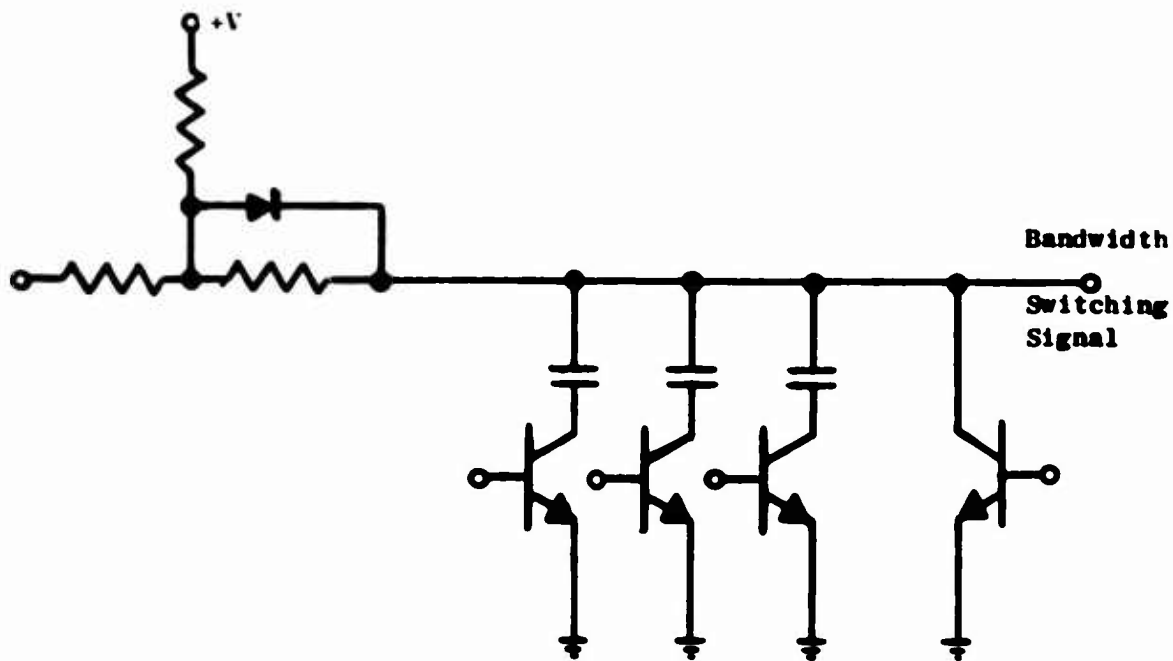


Fig. 25. BANDWIDTH SWITCHING CONFIGURATION.

Frequency conversion is another practical feature of this N-path filter. Operation as a selective frequency converter is possible when

$$f_{in} = nf_0 \text{ where } f_0 = \text{switching frequency and}$$

$$n = 1, 2, 3, \dots \text{ but } n \neq N, 2N, 3N, \dots$$

Then the output frequency may be chosen arbitrarily within the ranges

$$f_{OUT} = mf_0 \text{ where } m = 1, 2, 3, \dots$$

$$\text{but } m \neq N, 2N, 3N, \dots$$

Thus, the circuit can be used with the same switching frequency for various frequency bands.

Some design considerations which effect this circuit have been discussed earlier and in the literature [1A2].

1. Switching noise caused by phase and amplitude inequalities of the switching pulses

2. Signal-to-noise ratio can not be improved by increasing the signal voltage.
3. Although the switching noise can be eliminated by synchronizing the switching frequency with the signal, a certain minimum unsynchronized signal-to-noise ratio must be attained or problems will arise in the synchronizing circuit.

Experimental results for a prototype receiver with an AM bandwidth of 6 kHz and 200 kHz for FM, diode-tuned front end sections for AM and FM reception, and a digital discriminator are summarized below:

- | | |
|---|--|
| 1. Adjacent-channel selectivity | better than 46 dB |
| 2. Signal-to-noise ratio (non-synchronized) | approx. 30 dB |
| 3. Signal-to-noise ratio (synchronized) | dependent on front end |
| 4. Temperature stability (0 - 50°C) | ±500 Hz (dependent on switching pulse generator) |

Thus it can be seen from the above example that this configuration for a radio receiver makes it possible to integrate a good deal of the circuitry with very good results.

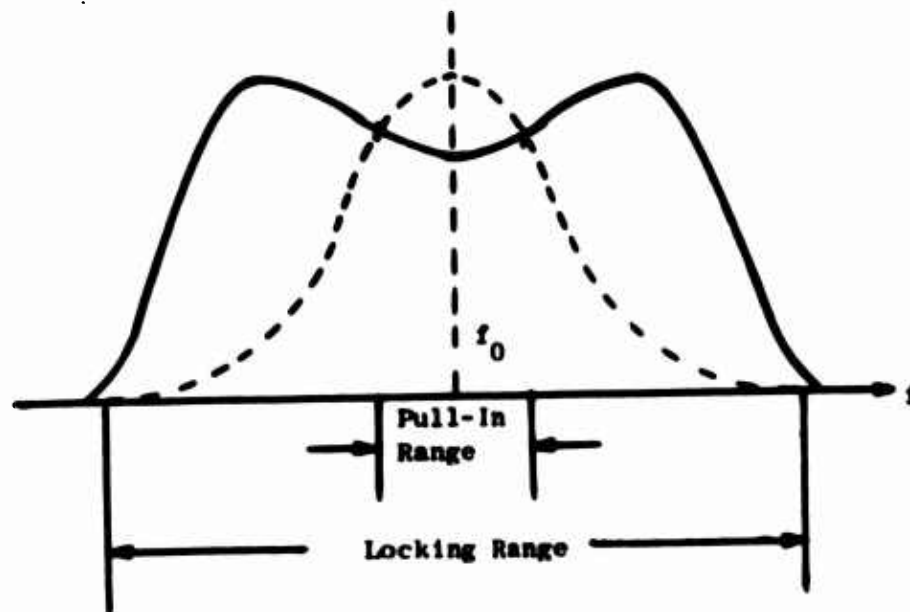


Fig. 26. VARIABLE BANDWIDTH CHARACTERISTIC OF FILTER RESPONSE.

BLANK PAGE

Chapter VII

CONCLUSIONS

A concerted effort has been made to bring together the theoretical background, the realization problems and a discussion of potential applications of the N-path filter in a continuous flow of ideas.

Early in this paper the transfer function was derived with Laplace transforms for generalized modulation, as well as, sinusoidal and rectangular. The low-pass to band-pass transformation form of the transfer functions were noted and discussed. From the view point of circuit integration, the rectangular modulation appears to be the most practical since the modulators can be replaced by series-sampling switches, and in some cases shunt-sampling may be employed.

Also considered was the effect of introducing other than low-pass elements in each path from a theoretical view. These require further investigation before a practical realization can be achieved. Study must be given to the circuit configuration, in each case, to minimize component tolerance effects and inter-path modulation errors as a minimum.

The remainder concerned itself singly with the low-pass to band-pass realization problems, since this application seems to have immediate interest. The effects of using non-ideal components are derived and analysed, circuit configurations to minimize these effects were proposed and an application was cited using one of these configurations.

This approach has many advantages even after consideration of the realization problems. It is a prime candidate for integration, it permits frequency response adjustment by adjusting the switching frequency, bandwidth may be varied electronically, it is capable of continuous operation over the range of 3 Hz to 3 MHz limited only by the switching transistors, and it offers high Q over all of its operating range without the use of inductors. Some of the disadvantages are: component tolerance becomes more critical as the number of paths increases, switching transistor matching becomes more critical as the switching frequency is increased, and switch driving signal phasing also becomes more critical as the frequency of the switching increases.

The advantages and short comings of the N-path filter discussed above are generally true and more specifically applicable to the circuit configuration used in the applications example. As technology in the integrated circuit, and thick and thin film areas advance, it is quite conceivable that component tolerances will decrease, transistors will improve and be better matched, the upper frequency limit will increase and the number of paths that can be applied will also increase.

The cost of implementing this type of device remains high. It is high for three reasons, first, because of the lack of sufficient technology to minimize the realization problems, secondly, the lack of more than a few papers which concern themselves with the realization problems, and finally, the lack of any knowledge in the majority of the design engineering community of the circuit configuration and its theoretical and potentially useful characteristics.

Appendix 1

LAPLACE TRANSFORM PAIRS

The following Laplace Transform pairs have been employed as necessary throughout the derivations within this paper.

$$x(t) \cdot y(t) \leftrightarrow X(s) \cdot Y(s) \quad (\text{A.1})$$

$$x(t) * y(t) \leftrightarrow X(s) \cdot Y(s) \quad (\text{A.2})$$

$$\exp[at] \leftrightarrow \frac{1}{s-a} \quad (\text{A.3})$$

$$t^n h(t) \leftrightarrow (-1)^n H^n(s) \text{ where } H^n(s) = \frac{d^n}{ds^n} [H(s)] \quad (\text{A.4})$$

$$\int_{-\infty}^{\infty} h(\tau)g(t-\tau) d\tau \leftrightarrow H(s)G(s) \quad (\text{A.5})$$

$$\int_{-\infty}^{\infty} h(\tau)g(t-\tau)\tau^n(t-\tau)^m d\tau \leftrightarrow (-1)^n(-1)^m H^n(s)G^m(s) \quad (\text{A.6})$$

$$h(t) \exp[-j\omega_0 t] \leftrightarrow H(s + j\omega_0) \quad (\text{A.7})$$

$$h(t) \exp[j\omega_0 t] \leftrightarrow H(s - j\omega_0) \quad (\text{A.8})$$

The following equality was also used in the derivations

$$F(s) * \frac{1}{s-a} = F(s-a) \quad (\text{A.9})$$

BIBLIOGRAPHY

- AC1 A. Acampora, B. Rabinovici, and C. A. Renton, "Generation of Bandpass Filters by Switching Techniques," Proc. IEEE (correspondence), vol. 51, pp. 256-257, Jan 1963.
- AC2 A. Acampora, "The Generalized Transfer Function and Pole-Zero Migrations in Switched-Networks," RCA Review, pp. 245-262, Jun 1966.
- BA1 N. F. Barber, "Narrow Band-Pass Filter Using Modulation," Wireless Engineer, vol. 24, p. 132, May 1947.
- BA2 D. R. Barber and M. J. Gingell, "Polyphase Modem for Frequency-Division Multiplex," Elec. Commun., vol 44, No. 2, pp. 108-114, 1969.
- BR1 B. Broeker, "Want a Bandpass Filter?," Elec. Design, pp. 76-78, Oct 25, 1970.
- DA1 S. Darlington, "Introduction to Time-Variable Networks," Proc. of Symposium on Circuit Analysis, p. 5-1, Urbana, Ill., Univ. of Ill., 1955.
- DA2 S. Darlington, "Some Circuits for Single-Sideband Modulation," Proc. Princeton Conf. Inform. Sys. Sci., pp. 66-70, 1969.
- FI1 R. Fischl, "Analysis of a Commutated Network," IEEE Trans. Aero. and Nav. Elec., pp. 114-123, Jun 1963.
- FR1 L. E. Franks and I. W. Sandberg, "An Alternative Approach to the Realization of Network Transfer Functions: The N-Path Filter," BSTJ, pp. 1321-1350, Sep 1960.
- FR2 L. E. Franks and F. J. Witt, "Solid Sampled Data Band-Pass Filters," Proc. 1960 Solid-State Circuits Conf., Phila., Pa.
- GL1 A. B. Glaser, C. C. Halkias and H. E. Meadows, "A Tuneable, Bandwidth-Adjustable Solid State Filter," Jour. Franklin Inst., vol. 288, pp. 83-98, Aug 1969.
- GL2 A. B. Glaser, "Digital Time-Division Multiplexed N-Path System," IEEE Trans. CT, vol. CT-17, pp. 600-604, Nov 1970.
- HA1 W. R. Harden, "Digital Filters with IC's Boost Q Without Inductors," Electronics Circuit Designer's Casebook, No. 1-4-7, pp. 114-123, McGraw-Hill.

- LA1 E. Langer, "Zeitmultiplexverfahren zur Filtersynthese," Frequenz, Bd. 20 (1966), Nr. 12, pp. 397-406.
- LA2 E. Langer, "Realisierungsprobleme bei N-Pfad-Filtern," Frequenz, Bd. 22 (1968), Nr. 1, pp. 11-16.
- LA3 E. Langer, "Ein Neuartiges N-Pfad-Filter mit zwei Konjugiert Komplexen Polpaaren," Frequenz, Bd. 22 (1968), Nr. 3, pp. 90-95.
- LA4 E. Langer, "Tune in With a New N-Path Filter," The Electronic Engineer, pp. 62-66, Nov 1969.
- LE1 W. R. LePage, C. R. Cahn and J. S. Brown, "Analysis of a Comb Filter Using Synchronously Commutated Capacitors," AIEE Trans. Communication and Electronics, vol. 72, pp. 63-68, Mar 1953.
- L11 W. K. Linvill, "The Use of Sampled Functions for Time-Domain Synthesis," Proc. Nat. Elec. Conf., Chicago, vol. 9, 1953.
- MA1 I. F. MacDiarmid and D. G. Tucker, "Polyphase Modulation as a Solution of Certain Filtration Problems in Telecommunications," Proc. IEE, vol. 97, Pt. 3, p. 349, Sep 1950.
- MA2 G. B. Madella, "Single-Phase and Polyphase Filtering Devices Using Modulation," Wireless Engineer, vol. 24, p. 310, Oct 1947.
- MO1 V. K. Mohrman and W. Hienlein, "N-Pfad-Filter Hoher Selektivitat mit Spulenlosen," Frequenz, Bd. 21 (1967), Nr. 12.
- PA1 H. B. Paris, Jr., "Utilization of the Quadrature Functions as a Unique Approach to Electronic Filter Design," IRE International Conv. Rec., Pt. 9, pp. 204-216, 1960.
- R11 G. A. Rigby, "Integrated Selective Amplifiers Using Frequency Translation," IEEE J. Solid-State Circuits, vol SC-1, pp. 39-44, Sep 1966.
- SA1 R. P. Sallen and E. L. Key, "A Practical Method of Designing RC Active Filters," IRE Trans. CT, pp. 74-85, Mar 1955.
- SM1 B. D. Smith, "Analysis of Commutated Networks," IRE Trans. Aero. Elec., vol. AE-10, pp. 21-26, Dec 1953.
- SU1 Y. Sun and I. T. Frisch, "A General Theory of Commutated Networks," IEEE Trans. CT, vol. CT-16, Nov. 4, pp. 502-508, Nov 1969.

- SC2 Y. Sun, "Network Functions of Quadrature N-Path Filters,"
IEEE Trans. CT, vol. CT-16, No. 4, pp. 594-600, Nov 1970.
- TH1 J. Thompson, "RC Digital Filters for Microcircuit Bandpass
Amplifier," EEE, pp. 45-49, 108, Mar 1964.
- TR1 J. G. Truxal, Automatic Feedback Control System Synthesis,
McGraw-Hill Book Co., Inc., New York, p. 221, 1955.
- WE1 D. K. Weaver, Jr., "A Third Method for Generation and
Detection of Single-Sideband Signals," Proc. IRE, vol.
44, p. 1703, Dec 1956.